SCIENCE CHINA Materials

REVIEW

mater.scichina.com link.springer.com

Published online 26 July 2016 | doi: 10.1007/s40843-016-5091-1
Sci China Mater 2016, 59(7): 589–608

Thin-film organic semiconductor devices: from flexibility to ultraflexibility

Yan Qian[1], Xinwen Zhang[1], Dianpeng Qi[2], Linghai Xie[1], Bevita K. Chandran[2], Xiaodong Chen[2*] and Wei Huang[1,3*]

ABSTRACT Flexible thin-film organic semiconductor devices have received wide attention due to favorable properties such as light-weight, flexibility, reproducible semiconductor resources, easy tuning of functional properties via molecular tailoring, and low cost large-area solution-procession. Among them, ultraflexible electronics, usually with minimum bending radius of less than 1 mm, are essential for the development of epidermal and bio-implanted electronics, wearable electronics, collapsible and portable electronics, three dimensional (3D) surface compliable electronics, and bionics. This review firstly gives a brief introduction of development from flexible to ultraflexible organic semiconductor electronics, and design of ultraflexible devices, then summarizes the recent advances in ultraflexible thin-film organic semiconductor devices, focusing on organic field effect transistors, organic light-emitting diodes, organic solar cells and organic memory devices.

Keywords: flexible electronics, organic field effect transistors, organic light-emitting diodes, organic solar cells, organic memory devices

INTRODUCTION

Organic electronics have received increasing attention due to favorable properties such as light-weight, flexibility, reproducible semiconductor resources, easy tuning of properties via molecular modification, and, most importantly, low cost, high throughput and large-area solution-processable fabrication techniques which are compatible with screen printing, ink jet printing and roll-to-roll coating techniques. Organic functional electronic devices, employing organic small molecule or polymer-based active semiconductors, mainly include organic field effect transistors (OFETs), organic light-emitting diodes (OLEDs), organic solar cells (OSCs), organic memory devices (OMDs), and so on. The active semiconductors can be organic channel materials for OFETs, organic light-emitting materials for OLEDs, organic photoactive materials for OSCs, organic memory materials for OMDs. To date, great improvements have been made for achieving high performance that is comparable to their inorganic counterparts [1–18].

However, most of these flexible devices exhibit minimum bending radius (R_b) of more than 1 mm, which easily causes bending-induced damages unless carefully protected. This significantly limits their practical applications for requirements of high durability and robustness such as intensely packed collapsible and portable electronics, wearable electronics, epidermal and bio-implanted electronics, and mechanically three dimensional (3D) surface compliable in-door and out-door devices, and bionics [19–27]. For such applications, ultraflexibility ($R_b \leq 1$ mm), for intimate conformabilities with the surfaces of arbitrary complex-shaped static and moving objects, is required so that the devices can survive repeated crumpling, creasing, sharp folding, or even stretching.

In this review, the development from flexible to ultraflexible organic semiconductor electronics, and design of ultraflexible devices were firstly introduced briefly. Then, the recent advances of ultraflexible functional electronic devices based on organic semiconductors were summarized, focusing on OFETs, OSCs, OLEDs and OMDs. Some of the significant developments were depicted in Fig. 1. Other ultraflexible electronic devices, utilizing one or more organic

[1] Key Laboratory for Organic Electronics and Information Displays & Institute of Advanced Materials (IAM), Jiangsu National Synergistic Innovation Center for Advanced Materials (SICAM), Nanjing University of Posts & Telecommunications, Nanjing 210023, China
[2] School of Materials Science and Engineering, Nanyang Technological University, Singapore 639798, Singapore
[3] Key Laboratory of Flexible Electronics (KLOFE) & IAM, Jiangsu National Synergistic Innovation Center for Advanced Materials (SICAM), Nanjing Tech University, Nanjing 211816, China
* Corresponding authors (emails: chenxd@ntu.edu.sg (Chen X), iamwhuang@njupt.edu.cn (Huang W))

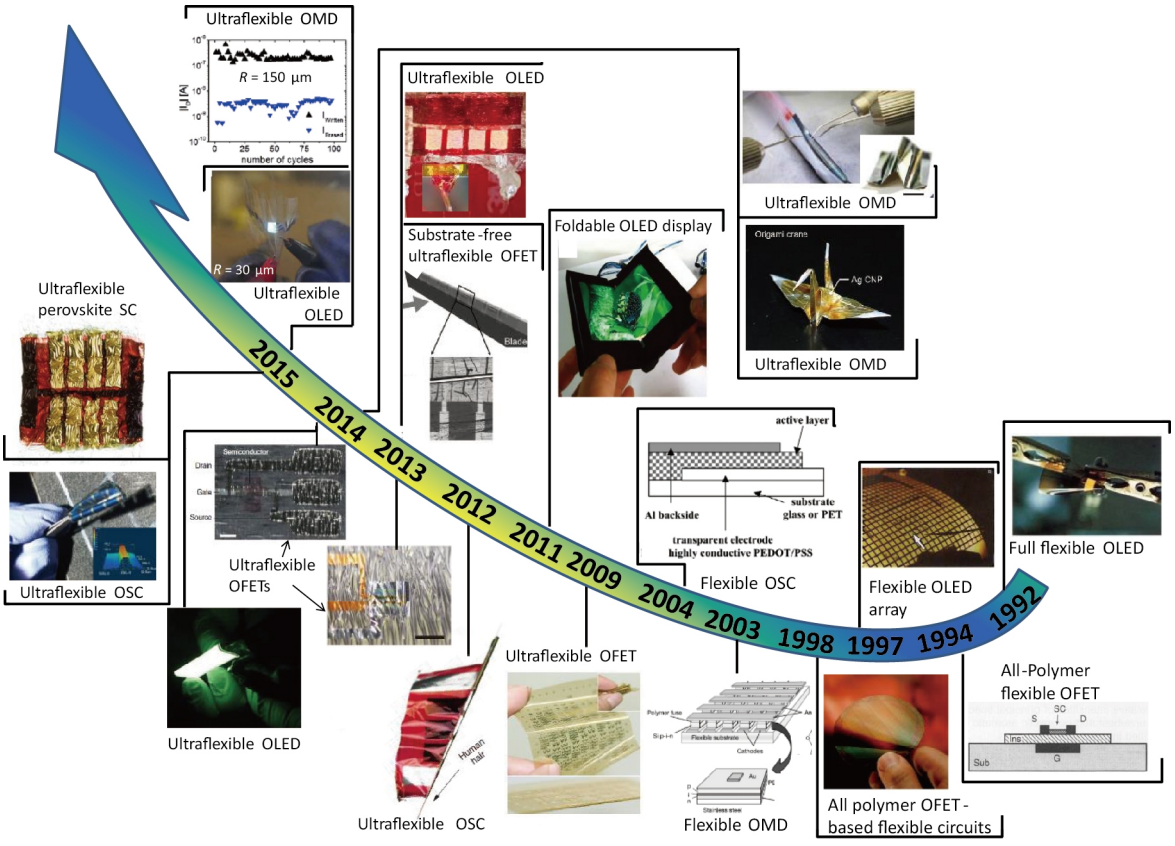

Figure 1 The development from flexible to ultraflexible organic semiconductor devices (OLED: organic light-emitting diode, OFET: organic field effect transistor; OSC: organic solar cell; OMD: organic memory device).

elements, such as sensors [28,29] and organic electrochemical transistor [30], are not included here, and interested readers are directed to other excellent articles on these subjects.

DEVELOPMENT FROM FLEXIBLE TO ULTRAFLEXIBLE ORGANIC SEMICONDUCTOR ELECTRONICS

Brief history of flexible organic semiconductor devices

Since Heeger's group [31] developed the first full flexible polymer-based OLED on polyethylene terephthalate (PET) substrate in 1992, flexible organic semiconductor electronics have widely received great attentions in scientific communities. In 1994, the first all polymer flexible OFET was developed by Garnier and coworkers [32] using printing techniques. Based on this, flexible OLED array [33] and circuit matrix [34] have been reported, respectively. In 2003, the first organic write-once read-many-times memory device was demonstrated by Forrest's group [35]. In 2004, Aernouts and coworkers [36] used highly conductive poly(3, 4-ethylenedioxythiophene)/poly(4-styrenesulfonate) (PEDOT:PSS) as a flexible transparent anode to fabricate flexible organic solar cell modules. In the last decades, high-performance flexible organic semiconductor devices have been continually pursued by scientific communities [16,37–48]. For example, OLEDs with external quantum efficiency (EQE) of >30% for blue [1–4] and green [5–9] emitting devices, and>20% for red [49] emitting devices, OSCs [10,11] and organic-inorganic hybrid perovskite solar cells [12] with power current efficiency (PCE) of >10% and 20%, respectively, OFETs with mobility of several tens $cm^2\ V^{-1}\ s^{-1}$ [13,14] and OMDs with high densities, high on/off ratios, fast response and long durability [15–18] have been reported.

Design of flexible organic semiconductor devices

Flexible device configurations

To fabricate flexible devices, utilization of the thin-film flexible substrates and/or electrodes is commonly adopted [50]. The flexible substrates usually are plastic platforms such as PET, polyimide (PI), polyethylene naphthalate

(PEN) and polycarbonate (PC). Other flexible substrates include textile [51,52], silk [53,54], paper [55–58], metal-foil [59,60], shape-memory polymer [61–63] and so on. Besides, weavable and fiber-like electrode [17,64]/device configurations [65–69], or even substrate-free free-standing configurations [70] are also demonstrated as effective ways for obtaining flexible devices. This review will focus on the thin-film organic semiconductor devices.

Design of flexible electrodes

As fundamental components of organic electronic devices, thin-film electrodes firstly need to be endowed with flexibility for fabrication of ultraflexible organic electronic devices. The flexible electrodes should exhibit little or even no change in conductivity at bending or folding states. The non-transparent flexible electrodes are mainly based on ductile metals such as Au and Al [37,39,40], and other conductors which are either dispersed in polymer matrix [31] or deposited onto flexible substrates [71]. However, for organic optoelectronic devices such as OSCs and OLEDs, in addition to high conductivity, high transparency is also demanded for efficient light transmittance. The most commonly used transparent electrode is indium tin oxide (ITO), due to its high conductivity for ensuring high performance as well as high transparency for efficient light penetration [72–74]. Although, flexible ITO-based devices such as OSCs [74,75], OLEDs [76,77] and OLECs [78,79] are reported, the intrinsic brittleness of ITO limits the further improvement of their flexibility for various applications. Therefore, it is essential to develop transparent, flexible, and conductive (TFC) electrodes to fabricate the ultraflexible organic optoelectronic devices.

For thin conducting films, sheet resistance (R_s) and transmittance (T) are linked through Equation (1) [80]:

$$T(\lambda) = \left(1 + \frac{188.5}{R_s}\frac{\sigma_{OP}(\lambda)}{\sigma_{DC}}\right)^{-2}. \quad (1)$$

To meet minimum industry standards, a conductive electrode with $\sigma_{OP}/\sigma_{DC} \geq 35$, corresponding to $T = 90\%$ and $R_s = 100\ \Omega$/sq, is generally demanded [80,81]. For the same electrode material, when R_s decreases, T simultaneously decreases. Therefore, the compromise between these two parameters should be reached to optimize the conductive films.

To date, the TFC electrodes are mostly based on PEDOT [36,70,74,82–98], graphene (GF) [73,75,99–112], carbon nanotubes (CNTs) [73,101,102,106–109,113], Ag-based nanowires/grids/films [72,114–125], copper nanowires [126] and ionic hydrogels [127], some of which exhibit good performances comparable to ITO electrodes (see Fig. 2). Correspondingly, some of optoelectronic devices using these TFC electrodes exhibit comparable performances to their ITO-based counterparts on rigid glass or flexible plastic substrates [45,70,72,74,75,83,87,88,101,103,118–120,128,129]. To further enhance the light extraction or light trapping in the devices, nanostructures or nanoparticles are introduced into these TFC electrodes for improving the device performances [47,130–140]. Besides these thin-film electrodes, fiber-/mesh-shaped electrodes also demonstrated good flexibility [17,51,64,67,68].

Fabrication of ultraflexible devices

It is known that a bending strain is defined by a function of $\varepsilon = h_s/(2R_b)$, where h_s is the substrate thickness and R_b is the bending radius [141]. Therefore, to reduce the bending strain at extreme bending states (corresponding to a very small R_b), ultra-thin substrate [60,96,97,123,124,139,142–148] or even substrate-free configurations [149–151] which reduce the total thickness of the devices and achieve ultraflexibility or extreme conformability, are generally employed.

Another consideration is to place a device at the neutral strain or neutral-plane position, i.e., the exact center along the film thickness direction where no strain is induced when the film is bent [26,27]. However, precise control of the thickness of the neighboring layers is difficult. In addition, because the actual thickness of a device is greater than zero, some parts of the device layers slip slightly from

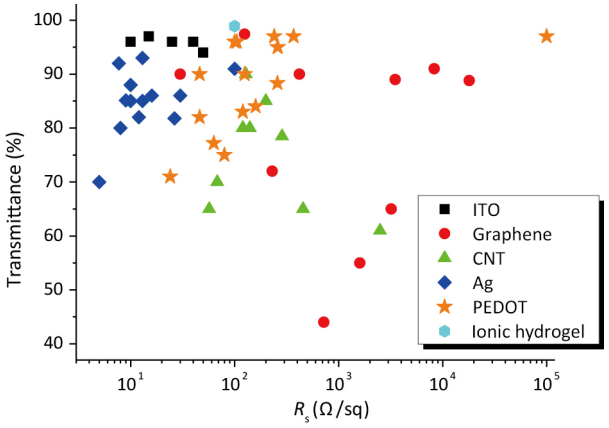

Figure 2 Transmittance at 550 nm (T_{550}) is plotted against sheet resistance (R_s) for ITO [72–75], PEDOT [70,74,82–89,96,97], Ag-based NWs/grid/film [72,114–120,123,124], CNTs [73,101,102,106–109], graphene [73,75,101–109] and ionic hydrogels [127].

the neutral-strain position, inevitably causing performance changes under strain. Therefore, this neutral-plane method is generally used as a complement to the design of the ultrathin device configuration [142,152].

ULTRAFLEXILBE ORGANIC SEMICONDUCTOR DEVICES

Ultraflexible organic field effect transistors

OFETs are basic building blocks for organic logic circuits and are essential for the development of printable and flexible electronic technologies [153,154]. For flexible OFETs, high performance includes high mobility, high on/off ratio, low operating voltage, fast response time and high yield in matrix arrays [37,40,155–158]. However, ultraflexible OFETs with minimum R_b less than 1 mm are rarely reported. To achieve ultraflexible OFETs, ultrathin substrates or dielectric layers are generally used. In 2005, Someya's group [142,152] fabricated an ultraflexible pentacene-based OFET with a mobility of 0.5 $cm^2 V^{-1} s^{-1}$ and an on/off ratio of 10^5, which remains functional at R_b of 0.5 mm. The key to realize the ultra-flexibility is to utilize the ultrathin substrate and encapsulation layers (both of 13 μm-thickness), with the transistors embedded at a neutral position. The sandwiched structure can drastically suppress strain-induced changes in transistor characteristics. No significant change was observed after 60,000 bending inward and outward cycles with R_b = 2 mm. When R_b decreases up to 0.5 mm, the mobility increases by 20% on inward bending stress, and decreases by 30% on outward bending stress.

Further efforts were put in developing bending-resistant OFETs at extreme bending states [159]. Someya [143] further improved the device structure to avoid this bending-induced damage in device performance. By using a 500-nm-thick atomically smooth planarization coating on ultrathin PI substrate, the surface root-mean-square (RMS) roughness decreases from 2.5 nm to 0.3 nm. Correspondingly, the resulting device can operate without degradation even being folded into a very small radius of 100 μm (Fig. 3). They developed imperceptible and ultraflexible OFETs with an ultra-dense oxide gate dielectric a few nanometers thick, which was fabricated directly on ultrathin (1.2 μm) PEN polymer foils (Fig. 4) [160]. These OFETs formed at room temperature enable sophisticated large-area electronic foils with unprecedented mechanical and environmental stability. They can withstand repeated R_b of 5 μm and less, can be crumpled like paper, accommodate stretching up to 230% on pre-strained elastomers, and can be operated at high temperatures and in aqueous environments. Based on OFET matrixes, applications include tactile sensor, thin-film heaters, temperature and infrared sensors and amplifiers have been demonstrated [160–162]. Another extremely flexible short-channel (channel length of 2 μm) OFET in a bottom-contact architecture has also been reported, which demonstrated excellent mechanical stability under systematic bending cycles at a R_b as small as 600 μm, and was durable against severe device crumpling [144]. Our group developed low voltage, air-stable, and ultraflexible pentacene-based OFETs using two layers of cross-linked PVP as the dielectric layer on a plastic PI substrate [163]. During a severe mechanical bending test (10^4 bending cycles with R_b = 0.75 mm) under ambient conditions, the OFETs still show excellent device performance at a low operational voltage. The variations of the electrical characteristics during the mechanical bending process were closely related to the distance effect of the spacing between stretched pentacene molecules as well as the doping effect of H_2O and O_2 induced by the mechanical bending strains.

Solution-processed suspended gate OFETs with minimum R_b of 250 μm which can be applied for ultra-sensitive pressure detection, has been reported by Zang *et al.* [164]. Fukuda's group [145] further developed a fully solution-processed highly flexible (with minimum R_b = 140 μm), extremely lightweight (2 g m^{-2}) and high performance OFET on 1-μm-ultrathick parylene-C films with high mobility (1.0 $cm^2 V^{-1} s^{-1}$), high on/off ratio (10^6), and fast operating speeds (~1 ms) at low operating voltages (10 V). The devices remained operational without significant changes in their performance, when tightly wrapped around a copper wire with R_b of 140 μm or even under 50% compressive strain. Without using substrates, a free-standing solution-processed OFETs, with 2 μm-thick Mylar layer serving as substrate-like insulation/dielectric layer, can tolerate multiple bending cycles without obvious degradation at a small R_b of 200 μm [150]. Moreover, highly crystalline solution-processed organic semiconductor films on thin plastic sheets result in high-performance with mobility up to 0.1–0.4 $cm^2 V^{-1} s^{-1}$. This free-standing dielectric layer strategy was also used to fabricate substrate-free OFETs via modified water-floatation method by Liu's group [165], which can be wrapped in close contact with the blade with the R_b of only 5 μm [151]. Moreover, sacrificial layers can be used to obtain ultraflexible OFETs [166]. The performance of these ultraflexible OFETs is summarized in Table 1.

By constructing the device on planar shape-memory sub-

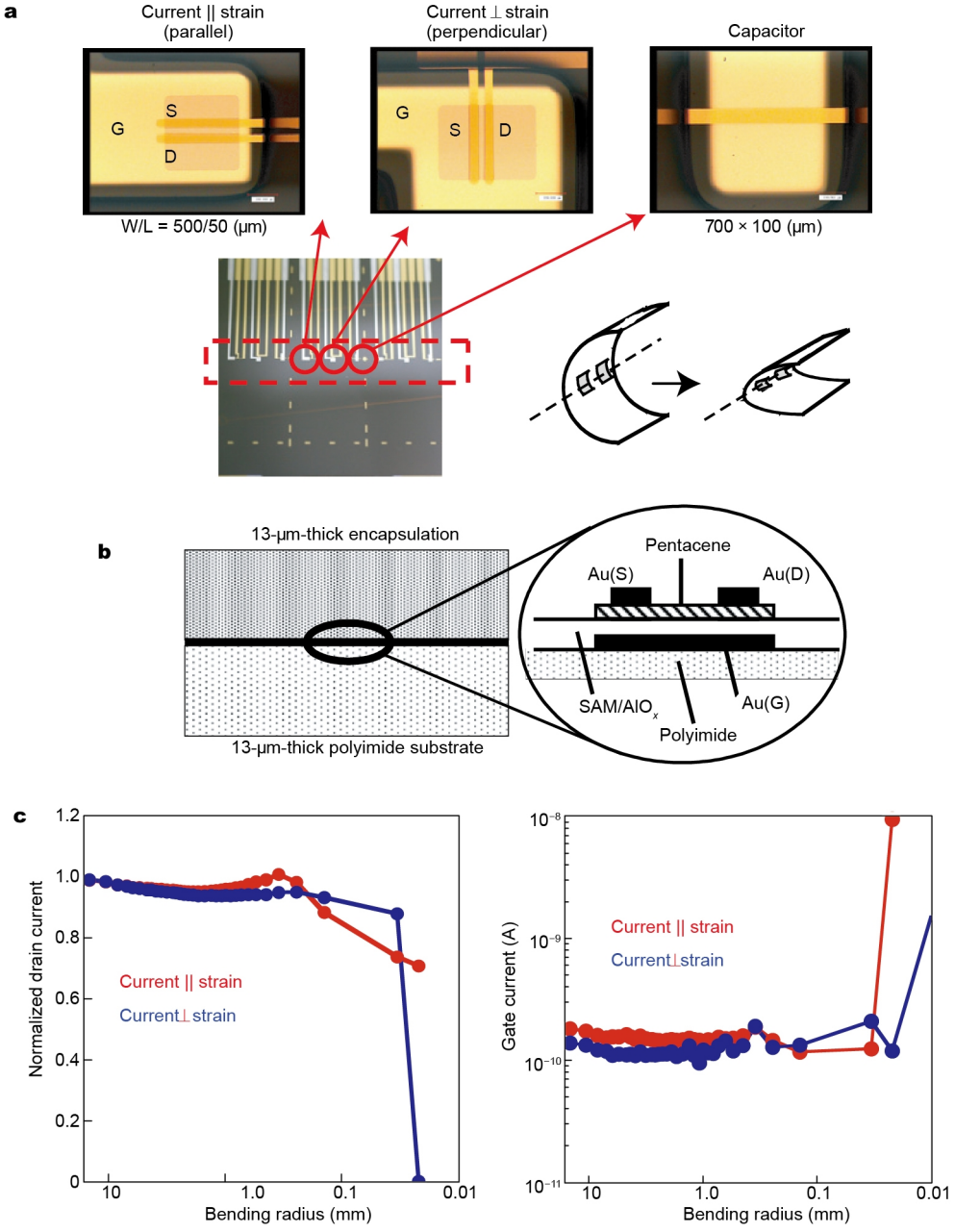

Figure 3 Bending tests on ultraflexible OFETs. (a) Photographs of an OFET in which the drain current flows parallel to the bending-induced strain, an OFET in which the current flows perpendicularly to the strain and an Al=AlO_x=SAM=Au capacitor that allows measurement of the gate dielectric capacitance during bending. The thin film transistors (TFTs) have a channel length of 50 μm and a channel width of 500 μm. The capacitor has an area of 700×100 μm^2. Bending was carried out using a custom-built precision bending apparatus. (b) Schematic illustration of the OFET configuration. (c) Left: measured drain currents of two pentacene OFETs (red: strain parallel to the drain current; blue: strain perpendicular to the drain current) as a function of R_b during inward bending, normalized to the initial drain current measured in the flat state. Right: gate currents of the same TFTs measured during inward bending. Drain-source voltage: −2 V; gate-source voltage: −2.5 V. Reprinted with permission from Ref. [143], Copyright 2010, Nature Publishing Group.

strates, a mechanically adaptive OFET can softly conform or deploy into 3D shapes after exposure to a stimulus with a small temperature change, which may find applications in implanted electronics [62]. Highly bendable OFET matrix was demonstrated on ultrathin parylene-C substrates using printed silver (Ag) nanoparticle interconnectors [145], on paper substrates assisted by a lithographic method [38,57], on mesh-like substrates [167] and even by substrate-free

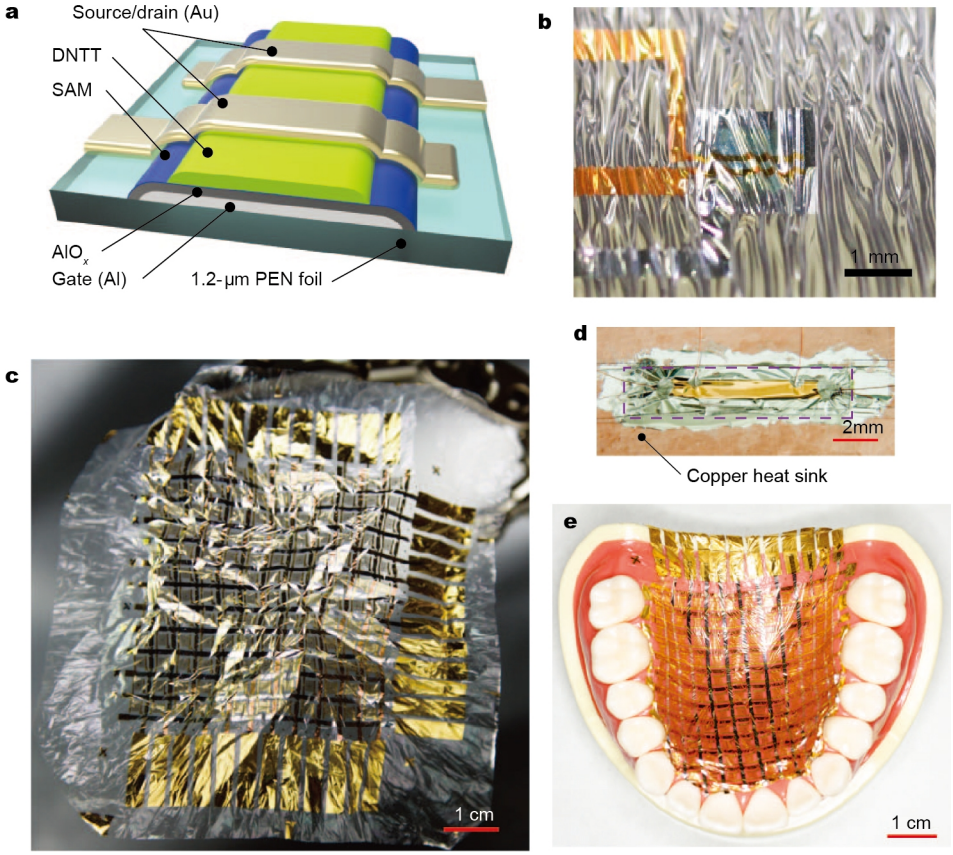

Figure 4 (a) Schematic ultrathin OFET on 1.2 μm PEN foils; (b) image of the stretch-compatible ultraflexible transistors; (c) imperceptible electronic foil of a thin large-area active-matrix sensor with 12×12 tactile pixels. (d) Thin-film infrared sensor with heat management-metallic conductors (100 nm Au) on a 1.2 μm PEN foil is placed on a Teflon support with low thermal conductivity which is then put on a copper block serving as heat sink. (e). Active-matrix tactile sensing foil sheet tightly conforming to a model of the human upper jaw. Reprinted with permission from Ref. [160], Copyright 2013, Nature Publishing Group.

Table 1 The device performance of ultraflexible OFETs; μ: field-effect mobility; on/off: on/off ratio; V_{on}: Operating voltage; $R_{b,m}$: minimum R_b

Active material/substrate (thickness)	μ (cm^2 V^{-1} s^{-1})	on/off	V_{on} (V)	$R_{b,m}$ (μm)	Ref.
Pentacene/PI (70 μm)	0.46	10^5	−4	750	[163]
Pentacene/PI (13 μm)	0.5	10^5	40	500	[142]
PDPP3T[a]/PET (25 μm)	0.34	10^4	- [b]	250	[164]
TIPS-pentacene/Mylar (2.5 μm)[c]	0.1–0.4	- [b]	- [b]	200	[150]
Fluoropolymer[c]/parylene-C(1μm)	1.0	10^6	10	140	[145]
Pentacene/PI (12.5 μm)	0.5	- [b]	2	100	[143]
PDI-C8/PAN&PS (320nm)[c]	0.23	- [b]	8.5	5	[151]
DNTT/parylene (60 nm)[d]	0.34	10^5	−1.72	2	[166]
DNTT/PEN (1.2 μm)	1.6	10^8	3	5~crumpling	[160]
DNTT/parylenediX-SR (1μm)	0.2	10^6	1	crumpling	[144]

a) Solution-processable; b) not available; c) with a freestanding gate insulator/dielectric layer; d) with an encapsulation layer

freestanding method [70]. Foldable OFET arrays applicable on both plastics and glass can be realized by using engineered substrates with nonuniform thickness, with thin areas for easy folding and thick areas for easy handling [168].

Ultraflexible organic solar cells

With fast development of renewable energy sources, the power efficiencies of OSCs have achieved as high as >10% [10,11]. With TFC electrodes, flexible OSCs can be ob-

tained by fabricating the devices on plastic substrates. Introducing nanostructures or nanoscattered particles into the devices may further enhance the light scattering and/or light trapping, and eventually improve the OSC efficiencies [136–140]. Based on the printed single wall carbon nanotube (SWCNT) film electrode on 125 μm-thick PET substrate with a T_{550} of 85% and a R_s of 200 Ω/sq, Rowell *et al.* [101] fabricated efficient, flexible polymer-fullerene bulk-heterojunction solar cells with comparable PCE ~2.5% with the ITO/glass-based counterparts (PCE = 3%). These devices could be bended to radius of 1 mm with a 20% ~ 25% loss in efficiency, and radius of 5 mm with no degradation in PCE.

By further reducing the thickness of the plastic substrate, devices with higher flexibility but reduced efficiency at bending state can be obtained. An ultraflexible polymer-based OSC on a very thin (1.4 μm-thick) and buckled plastic PET foil substrate was first demonstrated by Kaltenbrunner *et al.* [96]. The total thickness of the device is only 1.9 μm, which is even thinner than a typical thread of spider silk, resulting in an unprecedented lightweight (4 g m^{-2}). In addition to good stretchability due to buckled device configuration, the device can withstand extreme mechanical deformation, which can be demonstrated by wrapping around a human hair with a radius of 35 μm and deforming the cell on an elastomeric substrate with a plastic tube of 1.5 mm tip diameter (Fig. 5). More importantly, the device exhibits nearly identical PCE (4.2%) to their glass-based counterparts. Further by employing the organolead halide perovskites as the photoactive layer, they improved the PCE up to 12% [97].

Jung *et al.* [124] reported a flexible OSC exhibiting almost no degradation in device performance even after being folded with a radius of 200 μm, applying extremely bendable TFC electrode consisting of a Ag-grid-embedded ultrathin plastic substrate coated with ultrathin transparent ITO (T_{550} = 93%, R_s = 13 Ω/sq, R_b = 200 μm). The device showed a very small decrease of PCE (< 2.7%) at R_b = 200 μm, and excellent durability under repeated bending, exhibiting almost no change in its *J*–*V* characteristics even after 1000 bending cycles with R_b of 1.0 mm (Fig. 6). Based on consecutively stacked layers of conductive polymer (CP)-silver nanowires (AgNWs) composite belts fully embedded in a 20 μm-thick colorless PI (cPI) matrix, Kim *et al.* [123] fabricated a highly conductive (R_s = 7.7 Ω/sq) and transparent (T > 92% at wavelengths of 450–700 nm) electrode demonstrating a high flexibility and good mechanical durability with change of R_s less than 5% at outward bending and 10% at inward bending with R_b of 40 μm. Using this electrode, ultraflexible OSC that exhibits small PCE reduction of 5% when extremely bent at R_b = 40 μm can be fabricated. Moreover, the OSC achieves a much higher PCE (7.42%) than those based on electrodes simply embedding AgNWs without CP in cPI, possibly due to a

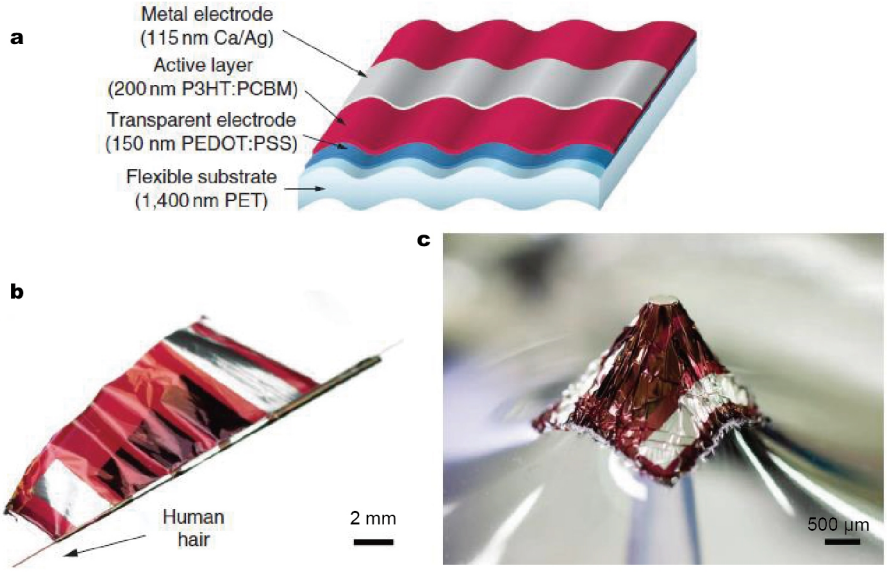

Figure 5 Stretchable and compressible 2 μm-thick OSC on ultrathin PET substrate: (a) scheme of the ultra-light and flexible organic solar cell; (b) extreme bending flexibility demonstrated by wrapping a solar cell around a 35 μm-radius human hair; (c) the device attached to the elastomeric support, under three-dimensional deformation by pressure from a 1.5 mm-diameter plastic tube. Reprinted with permission from Ref. [96], Copyright 2012, Nature Publishing Group.

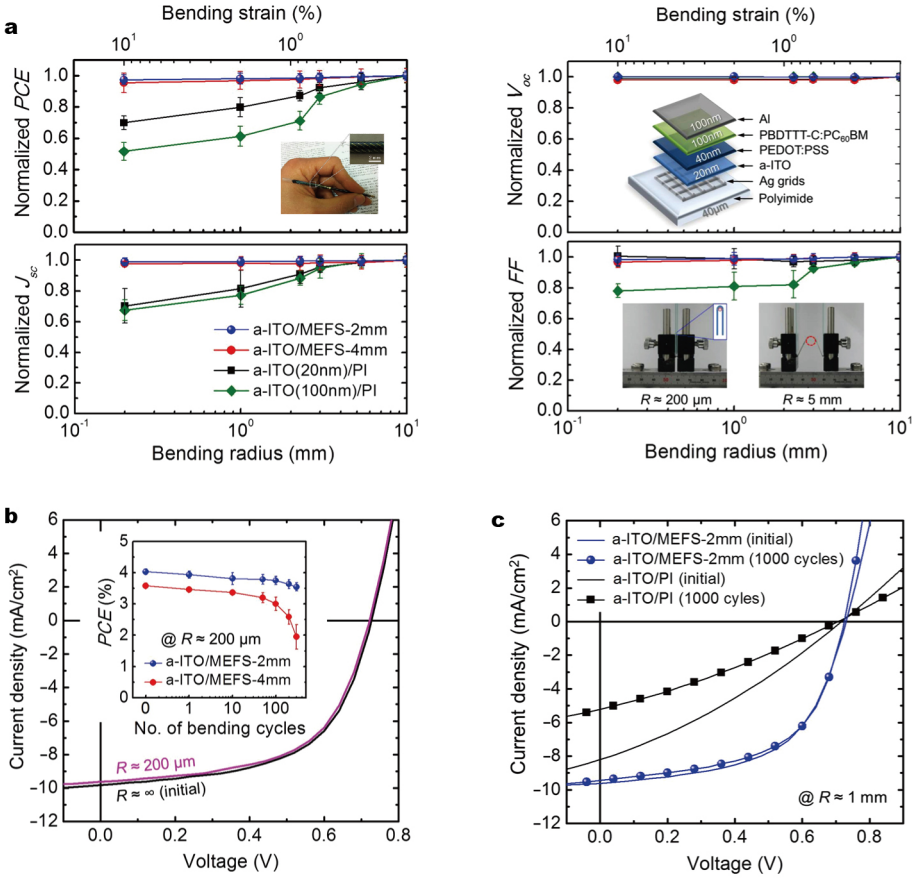

Figure 6 (a) Normalized PCE, V_{oc}, J_{sc}, and FF values of the flexible OSCs as a function of the R_b during compressive bending. The top left inset shows a photograph of a flexible OSC wrapped around a cylinder with a radius of ≈1 mm. The top right and bottom right insets show the device structure and the bending process of OSCs, respectively. (b) The current density-voltage characteristics measured in the flat and bend (with R_b of ≈200 μm) state, respectively. The measured PCE values as a function of the folding cycles at R_b ≈ 200 μm are shown in the inset. (c) The current density-voltage characteristics of the OSCs after being bent 1000 times with a R_b of ≈1 mm. Reprinted with permission from Ref. [124], Copyright 2014, WILEY-VCH.

Table 2 The electrode and device performance of ultraflexible and/or stretchable OSCs. R_s: sheet resistance; T_{550}: transmittance at 550 nm; R_b (ΔR_s): minimum bending radius (change of R_s at this R_b); PCE: power conversion efficiency; CP: conductive polymer, CPI: colorless polyimide; a-ITO: amorphous ITO

Electrode				OSC			Ref
Electrode/substrate[a]	R_s (Ω/sq)	T_{550} (%)	R_b (μm) /ΔR_s	Active layer	PCE (%)	R_b (μm) /ΔPCE	
SWCNTs/PET(125 μm)	200	85	1000/<25%	P3HT:PCBM	2.5	1000/20–25%	[101]
a-ITO(20 nm)/Ag-grid in PI (40 μm)	13	93	200/<10%	PBDTTTC:PCBM	4	200/<2.7%)	[124]
CP-AgNWs in cPI (20 μm)	7.7	92	40/<5%^{out},<10%^{in}	P2:PC_{71}BM	7.42	40/5%	[123]
PEDOT[b] (150 nm)/PET(1.4 μm)	100	96[c]	35/-[d]	P3HT:PCBM	4.2	35/-[d]	[96]
PEDOT[b] (130 nm)/PET(1.4 μm)	105	96[c]	10/-[d]	Perovskite MADI	12	10/-[d]	[97]

a) Thickness, if available, is indicated in the brackets; b) PEDOT:PSS electrodes:PH1000:5*v*.% DMSO:0.5. *v*.% Zonyl; c) from Ref [86]; d) not available

reduction in bimolecular recombination and an increased charge collection efficiency. In addtion, using organic acceptors instead of the traditional but brittle PCBM has been demonstrated as an effective way to enhance the mechanical robustness [169]. Kim's group demonstrated the mechanically robust all-polymer solar cells that were based on the PBDTTTPD:P(NDI2HD-T) donor-acceptor polymer system, with high PCE of 6.64%. The performances concerning the electrodes (T_{550}, R_s, R_b) and devices (PCE and R_b) are summarized in Table 2.

Ultraflexible organic light-emitting diodes

Ultraflexible OLEDs

Since Heeger and Forrest reported the first polymer- [31] and small molecule- [170] based flexible organic light-emitting OLED, respectively, high efficiency is always pursued in this field [135,171]. Based on this, flexible displays of OLED arrays are demonstrated [33,172]. To fabricate ultraflexible OLEDs, transparent TFC electrodes are required. The reported electrodes utilized in flexible OLEDs are mainly based on PEDOT [173], CNT [44,174], Ag NWs/grids [175–179], graphene [45,180], ITO [76], and metal oxide [181]. For achieving higher efficiency, top-emitting architectures [182–185] and nanostructured/scattered electrodes or substrates [47,130–135] can be adopted, to enhance output coupling or light extraction of the devices.

However, to achieve high flexibility, extremely bendable TFC electrodes firstly need to be developed [88,120,124,146,147,177,186]. Yu *et al.* [120] developed an AgNWs/shape-memory-polymer composite electrode deposited on PET substrate on which a flexible yellow OLED with minimum R_b of 2.5 mm has been constructed. The R_s of the electrode is almost the same under inward bending with compressive strain of 16%, but exhibits a significant increase of 290% under outward bending with tensile strain of 16%. For the OLED device, a slight change in the *I*-*V*-*L* responses was observed after 10 bending cycles with inward and outward R_b of 2.5 mm, and the maximum current efficiency (CE) remains constant at around 14 cd A^{-1}. Using such electrodes, they further fabricated a flexible blue bis(3,5-difluoro-2-(2-pyridyl)-phenyl-(2-carboxypyridyl) iridium(III) (FIrpic) based phosphorescent OLED reaching a maximum CE of 25 cd A^{-1}, which decreases to 18.3 cd A^{-1} after 100 bending-recovery cycles with R_b = 1.5 mm [187]. However, the use of shape memory polymers requires heat treatment for deformation, which limits their practical applications. Further, with no requirement of thermal treatment, they applied a composite electrode based on a thin AgNW network inlaid in thesurface layer of a rubbery poly(urethane acrylate) (PUA) matrix, and fabricated a bendable and collapsible polymer light-emitting diode (PLED) [147]. The device emitted light brightly and uniformly even, when wrapped around the edge of 400 μm thick cardboard. Bending or folding causes no mechanical or electrical damage to the device because of the high flexibility and conductivity of the AgNW–PUA composite electrodes.

Using the ultraflexible AgNW networks welded by the sputtered transparent conductive oxide, an ultraflexible OLED which can be bent to a radius of 1 mm has been demonstrated [128]. Jung *et al.* [124] reported an ultraflexible electrode by coating 20 nm α-ITO on a metal embedding flexible substrate, with the change in R_s being small (≈10%) even after bending with a R_b of ~200 μm (corresponding to a bending strain ε of 10%). The phosphorescent OLED (PhOLED) fabricated with this electrode also showed excellent mechanical flexibility, with the light-emitting intensity retaining ~94% of the original value even after the device was bent with R_b of ~200 μm (Fig. 7). Ultrathin (total thickness of 2 μm) buckled red and orange PLEDs fabricated on pre-strained 1.4 μm-thick PET foil with unprecedented flexibility with radius of curvature under 10 μm have been demonstrated by White *et al.* [146]. This foil-based electronics are to reversibly undergo folding, wrinkling, crumpling and twisting deformations, without catastrophic failure, and can be applied in surface-conforming thin-film electronics (Fig. 8). In addition, these buckled PLEDs exhibit favorable stretchability and compressibility, which can tolerate 100% tensile strain and 50% compress, respectively. Nagata *et al.* [88] developed a smooth, ultraflexible, and transparent electrode with AgNWs embedded in ultrathin (10 μm-thickness) cPI. This electrode film exhibits mechanical durability, for both outward and inward bending tests, up to a minimum R_b of 30 μm, while maintaining its electrical performance after 100,000 bending cycles at R_b = 500 μm. Blue PhOLEDs using these composites as bottom anodes show only slight performance reduction of 3% even after repeated folding with R_b of 30 μm. Yokota [188] recently reported an ultraflexible and conformable three-color, highly efficient PLEDs and organic photodetectors (OPDs) to realize optoelectronic skins that introduce multiple electronic functionalities such as sensing and displays. The performance of these ultraflexible electrodes and devices are summarized in Table 3.

Foldable OLED displays

Yun *et al.* [190] demonstrated a mean of providing stable and homogenous interfacial adhesion by using two-dimensional arrays of OLED posts, which tolerate the etching process and undergo cohesive fracture during transfer printing, to directly anchor the flexible substrate. Lee's group [191] reported a mechanically and optically robust folding structure composed of two individual OLED panels and a hyper elastic silicone rubber to realize a foldable and seamless active matrix OLED (AMOLED) display without a visible crease at the junction. The folding-unfolding test

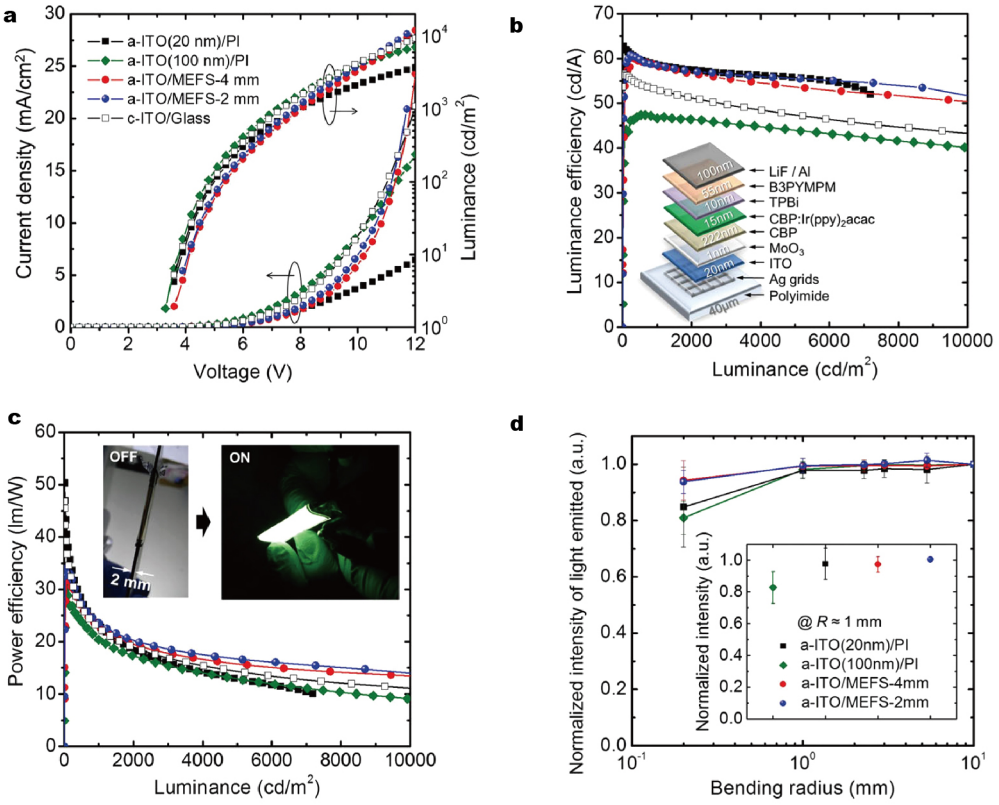

Figure 7 (a) Current density-voltage characteristics of the OLEDs fabricated using different transparent conducting electrodes. (b) Current efficiency-luminance characteristics of the OLEDs. The inset shows a schematic of the flexible OLEDs. (c) Power efficiency-luminance characteristics of the OLEDs. The inset shows photographs of the large-area bendable OLEDs (5×5 cm^2). (d) Measured intensity of the light emitted by the flexible OLEDs as a function of the R_b during compressive bending, normalized to the initial value. The inset shows the normalized light-emitting intensities measured after 1000 times of bending the OLEDs with a R_b of ~1 mm. Reprinted with permission from Ref. [124], Copyright 2014, WILEY-VCH.

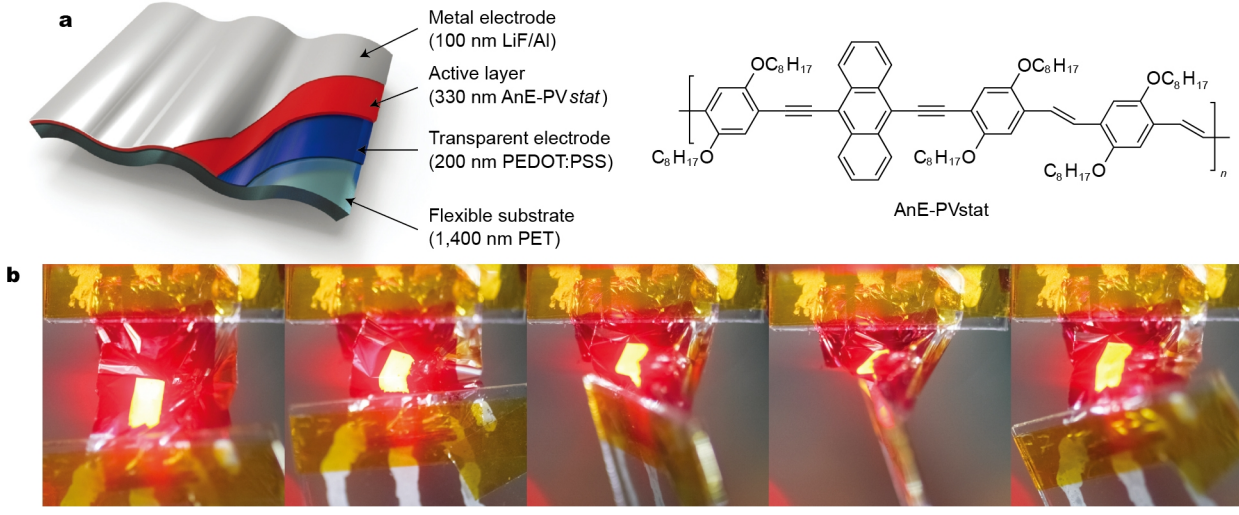

Figure 8 (a) Schematic of the ultraflexible PLEDs with each layer thickness drawn to scale. The schematic shows periodic bending with a radius of curvature of 5 μm for reference. The chemical structure of AnE-PVstat is shown at the right side. (b) Demonstrations of extreme deformation attainable with ultrathin PLEDs, with images of a free-standing ultrathin PLED operating during crumpling. The device is suspended between two pieces of glass that are moved closer together and simultaneously twisted by 90°. Each pixel is ~ 3 mm × 6 mm. Reprinted with permission from Ref. [146], Copyright 2013, Nature Publishing Group.

Table 3 The performance of the electrodes and devices for ultraflexible OLEDs (R_m: minimum bending ratio; CE: current efficiency; PE: power efficiency)

Electrode				OLED				Ref.
Anode/substrate[a]	R_s (Ω/sq)	T_{550} (%)	R_m (μm) /ΔR_s	Active layer	CE(cd A^{-1})	PE (lm W^{-1})	R_m (μm)	
a-ITO (20 nm)/Ag-grid in PI (40 μm)	13	93	200 /<10%	$Ir(ppy)_2(acac)$:CBP[b]	59	38	200	[124]
AgNW/PUA (150 μm)	15	83%	- [c]	SuperYellow:ETPTA: PEO: LiTf	1.0[d]	- [c]	200	[147]
AgNW/cPI (10μm)	8	80	30 /<3%	FIrpic: mcP[b]	21	7.4	30	[88]
PEDOT:PSS[e] /PET (1.4 μm)	135	95%	- [c]	AnE-PVstat	0.026[d]	- [c]	10	[146]
				MDMO-PPV	0.17[d]	- [c]		

a) Thickness, if available, is indicated in the brackets; b) emitter: host; c) not available; d) the device is also stretchable; e) PH1000:5 *v*.% DMSO: 0.5 *v*.% Zonyl

on the structure exhibited negligible deterioration of the relative brightness at the junction of the individual panels up to 105 cycles at a folding radius of 1 mm. They further adopted a top emission structure into the flexible OLED display device, composed of an OLED microcavity covered with thin film encapsulation, a low temperature color filter (LTCF), and an ultrathin (500 nm-thickness) PI substrate. This display demonstrates low power consumption, high outdoor readability, and resistance to moisture and oxygen in ambient atmosphere (Fig. 9) [189]. The variation of relative brightness is within 6% of the original brightness after folding 10,000 times with R_b = 1 mm. Moreover, even after soaking the panel in water for one hour, no variation in the OLED brightness is observed. Such ultrathin and flexible displays, by integrating with a touch sensor, may find good applications in touch screen in electronic devices [192], and visible pressure sensing in artificial skins [193,194].

Ultraflexible organic memory devices

High performance flexible OMDs, including organic resistors [195–200], OFET memories [16,39,201–208] and other complex-structured memories [209,210], are vastly investigated concerning high switching speed, high on/off ratios, long retention time, and even multi-level states or multi-functionalities [211]. They show tremendous applications in sensor arrays [212–214], braille displays [39], integrated circuits [215] and RFIDs [48]. However, the flexibility of most reported OMDs has been limited, with R_b mostly in millimeter range, due to the difficulty in maintaining memory characteristics while bending. Among various kinds of OMDs, the OFET memory is the most striking and has been widely investigated recently due to its nondestructive read-out property, single-transistor realization, and good compatibility with the complementary metaloxide semiconductor devices [216,217]. Kim *et al.* [218] demonstrated solution-processed non-volatile ferroelectric OFET memories operating in p- and n-type dual mode, which exhibit excellent mechanical flexibilities. They used ferroelectric poly(vinylidene fluoride-cotrifluoroethylene) (PVDF) as thin insulator layer and a quinoidal oligothiophene derivative ($QQT(CN)_4$) as organic semiconductor (Fig. 10). These dual-mode field-effect devices are highly reliable with data retention of 46,000 s and endurance of 100 cycles, respectively, even after 1,000 bending cycles with R_b of 4 mm. No significant decay in performance was observed after tens of multiple bending cycles with extreme R_b of 500 μm by hand, with sharp folding or even crumpling. The plasticity of $QQT(CN)_4$ and its firm interface with PVDF-TrFE plays a crucial role in resisting such extreme mechanical deformations. A highly bendable OFET memory on ultrathin PI substrate (13 μm-thickness) was reported by Cosseddu *et al.* [148,219], with negligible variation of the threshold voltage and transfer characteristics even after 200 cycles of bending at a R_b of 150 μm. Other device architectures including resistive memory diodes and some complicated structures have also been demonstrated in ultraflexible OMDs. Nagashima *et al.* [60] proposed ultraflexible resistive nonvolatile memories on ultrathin Al foil using Ag-decorated cellulose nanofiber paper as active layer, exhibiting high on/off resistance ratio of 10^6 and small standard deviation of switching voltage distribution. The memory performance can be maintained without any degradation when being bent down to the R_b of 350 μm. A twistable 8 × 8 cross-bar array-type organic nonvolatile resistive memory device on PET substrate, which well retains the device performance under the twisted condition with a twist angle up to 30°, has been reported [220]. Jeong *et al.* [209] demonstrated

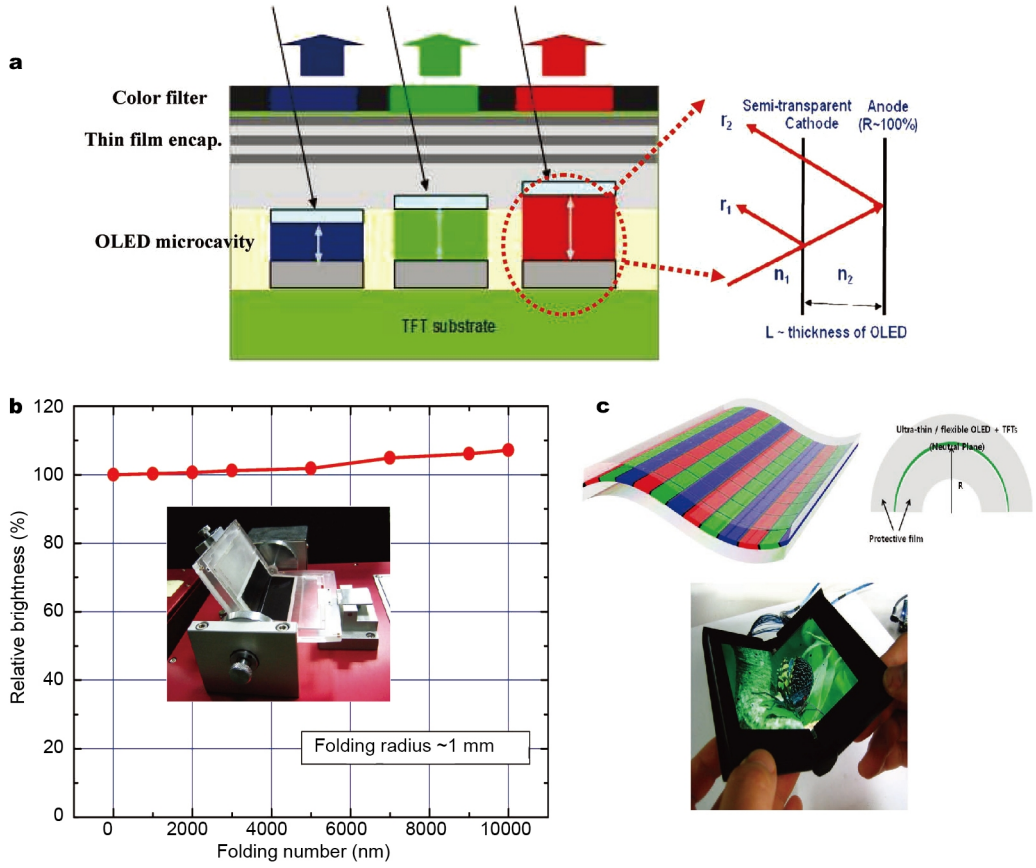

Figure 9 (a) Schematic view of a new optical system for a flexible display device composed of a LTCF, TFE, and a RGB OLED microcavity. Inset: the structure of the RGB microcavity: The different thicknesses of the RGB OLED layer are primarily designed to the optical length (L) of the RGB cavity to form a standing wave inside the optical resonator. To undergo fully destructive interference of reflective lights between the semi-transparent cathode and reflective anode, L of the OLED should be equal to an integer multiple of primary color (λ_n). (b) Optical measurement of a flexible OLED device after folding a 1 mm radius window module. Relative brightness is monitored in steps of 1000 folds for a total 10,000 folds. Inset: experimental setup for mechanical folding test. (c) Up: a schematic view of a neutral plane used to eliminate strain applied at a backplane and OLED device; bottom: a foldable and seamless OLED display fabricated by arranging two OLED panels and one transparent plane. The left OLED panel is slimmed down to 50 μm and assembled on the transparent plane. Reprinted with permission from Ref. [189], Copyright 2011, WILEY-VCH.

a flexible all-organic 64-bit memory cell array possessing one diode–one resistor architectures, which exhibits excellent rewritable switching characteristics, even during and after harsh physical stresses including bending, twisting and rolling. The write-read-erase-read output sequence of the cells perfectly corresponds to the external pulse signal regardless of substrate deformation, suggesting potentials of such device for applications in high-density flexible OMDs. The device performance, bending durability as well as device architectures are summarized in Table 4.

SUMMARY AND OUTLOOK

In general, the organic devices exhibit relatively poor device performance and durability in ambient atmosphere when compared to their inorganic counterparts. However, they have many advantages over the inorganic devices such as intrinsic flexibility, low cost of organic materials, the relaxed requirements of purity, the minute thicknesses of material required (≤100 nm), and relatively facile solution processability. To date, ultrathin flexible full-color AMOLED display with total thickness of 10 μm and minimum R_b of less than 1 mm has been demonstrated [221]. For further development, on the one hand, current efforts are aimed at improving the device efficiency and environmental stability to approach or even surpass their inorganic counterparts, so as to enable these organic devices to be widely adopted for practical and robust applications. On the other hand, integration of multifunctionalities in ultraflexible organic semiconductor devices is another research goal in scientific communities. This can be realized either by integrating with other individual functional devices or by integrating multiple functionalities by molecular design of organic

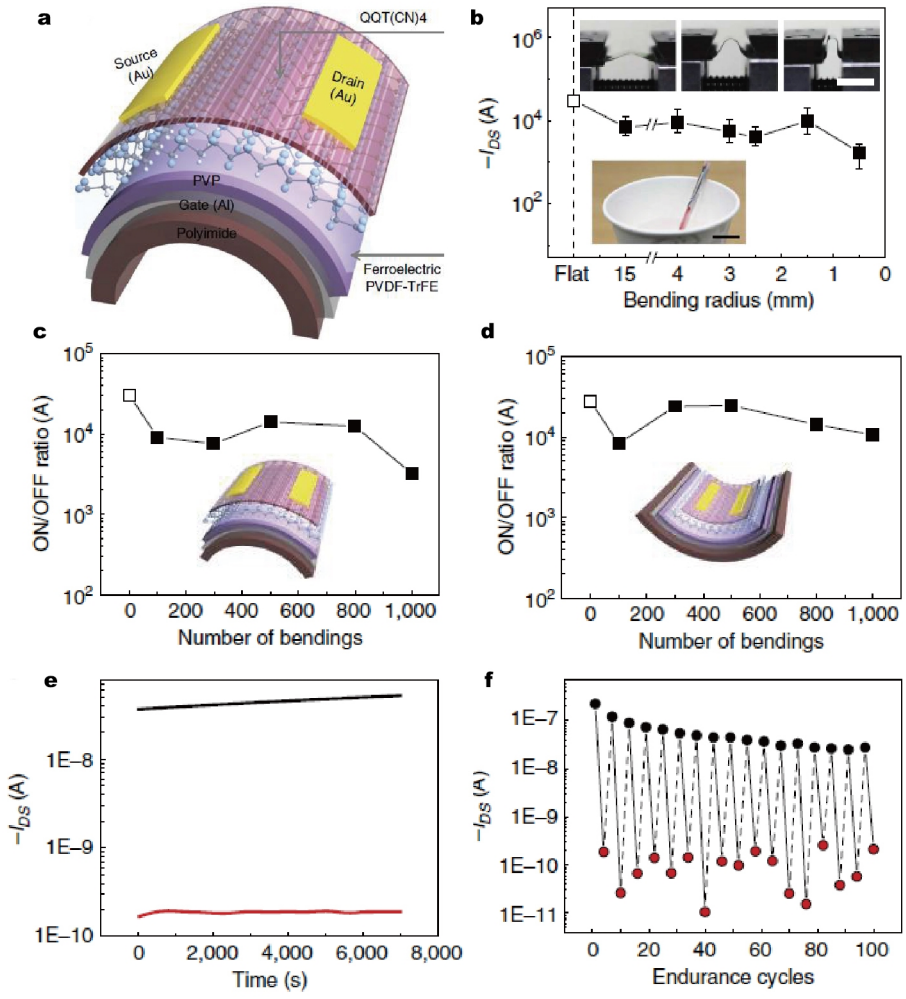

Figure 10 (a) Schematic representation of the p-type QQT(CN)$_4$Fe-based OFET memory devices. (b–f) Bending tests on ultraflexible organic Fe-FET memories: (b) on/off current ratio measured at V_{DS} = –5 V as a function of the R_b. The data were averaged with 10 devices examined for each R_b. Inset is a photograph of super-flexible devices rolled on a commercially available coffee stirrer with R_b of ~500 μm. (c, d) on/off current ratio measured at V_{DS} = –5 V as a function of the number of bending cycles in outward (c) and inward (d) directions with a R_b of 4 mm, respectively. Insets are the diagrams of inward and outward-bending devices, respectively. (e) Data retention characteristics measured after programming the device with single voltage pulses for the ON and OFF current after 1000 inward bending cycles at a R_b of 4 mm. (f) Write/erase endurance cycle test as a function of the number of programming cycles after 1000 outward bending cycles at a R_b of 4 mm. For clarity, one cycle out of every four is represented. The programming voltage pulses for switching ON and OFF states were –50 and +50 V, respectively. The read voltages for both ON and OFF states were V_G = –10 V and V_{DS} = –5 V. Reprinted with permission from Ref. [218], Copyright 2014, Nature Publishing Group.

Table 4 Device architectures and device performance of ultraflexible OMDs

Device architecture/substrate (thickness)	on/off	t_R (s)	$R_{b,m}$ (μm)	Ref.
1D–1R memory array[a]/PEN (125 μm)	10^3	10^4	1000[b]	[209]
FET memory/PI (100 um)	5×10^3	$>6\times10^3$	500~crumpling	[218]
FET memory/Al paper[b] (200 um)	5×10^3	$>6\times10^3$	~sharp folding	
Resistive memory/Al foil (12 μm)	10^6	10^5	350	[60]
FET memory/PI (13 μm)	10^2	3×10^5	150	[219]

a) 1D–1R: one diode–one resistor; b) Al coated PI substrate

semiconductors.

Received 28 June 2016; accepted 13 July 2016; published online 26 July 2016

1 Shin H, Lee S, Kim KH, *et al.* Blue phosphorescent organic light-emitting diodes using an exciplex forming Co-host with the external quantum efficiency of theoretical limit. Adv Mater, 2014, 26: 4730–4734
2 Kim M, Lee JY. Engineering the substitution position of diphenylphosphine oxide at carbazole for thermal stability and high external quantum efficiency above 30% in blue phosphorescent organic light-emitting diodes. Adv Funct Mater, 2014, 24: 4164–4169
3 Lee CW, Lee JY. Above 30% external quantum efficiency in blue phosphorescent organic light-emitting diodes using pyrido[2,3-*b*] indole derivatives as host materials. Adv Mater, 2013, 25: 5450–5454
4 Udagawa K, Sasabe H, Cai C, *et al.* Low-driving-voltage blue phosphorescent organic light-emitting devices with external quantum efficiency of 30%. Adv Mater, 2014, 26: 5062–5066
5 Sun JW, Lee JH, Moon CK, *et al.* A fluorescent organic light-emitting diode with 30% external quantum efficiency. Adv Mater, 2014, 26: 5684–5688
6 Kim SY, Jeong WI, Mayr C, *et al.* Organic light-emitting diodes with 30% external quantum efficiency based on a horizontally oriented emitter. Adv Funct Mater, 2013, 23: 3896–3900
7 Lee DR, Kim BS, Lee CW, *et al.* Above 30% external quantum efficiency in green delayed fluorescent organic light-emitting diodes. ACS Appl Mater Interfaces, 2015, 7: 9625–9629
8 Kim M, Lee JY. Engineering of interconnect position of bicarbazole for high external quantum efficiency in green and blue phosphorescent organic light-emitting diodes. ACS Appl Mater Interfaces, 2014, 6: 14874–14880
9 Liu J, Shi X, Wu X, *et al.* Achieving above 30% external quantum efficiency for inverted phosphorescence organic light-emitting diodes based on ultrathin emitting layer. Org Electron, 2014, 15: 2492–2498
10 You J, Chen CC, Hong Z, *et al.* 10.2% power conversion efficiency polymer tandem solar cells consisting of two identical sub-cells. Adv Mater, 2013, 25: 3973–3978
11 You J, Dou L, Yoshimura K, *et al.* A polymer tandem solar cell with 10.6% power conversion efficiency. Nat Commun, 2013, 4: 1446
12 Yang WS, Noh JH, Jeon NJ, *et al.* High-performance photovoltaic perovskite layers fabricated through intramolecular exchange. Science, 2015, 348: 1234–1237
13 Tseng HR, Phan H, Luo C, *et al.* High-mobility field-effect transistors fabricated with macroscopic aligned semiconducting polymers. Adv Mater, 2014, 26: 2993–2998
14 Yuan Y, Giri G, Ayzner AL, *et al.* Ultra-high mobility transparent organic thin film transistors grown by an off-centre spin-coating method. Nat Commun, 2014, 5:
15 Cho B, Song S, Ji Y, *et al.* Organic resistive memory devices: performance enhancement, integration, and advanced architectures. Adv Funct Mater, 2011, 21: 2806–2829
16 Baeg KJ, Khim D, Kim J, *et al.* High-performance top-gated organic field-effect transistor memory using electrets for monolithic printed flexible NAND flash memory. Adv Funct Mater, 2012, 22: 2915–2926
17 Dai MK, Lin TY, Yang MH, *et al.* High-performance organic nano-floating-gate memory devices based on graphite nanocrystals as charge-trapping elements and high-k Ta_2O_5 as a controlled gate dielectric. J Mater Chem C, 2014, 2: 5342
18 Wu W, Zhang H, Wang Y, *et al.* High-performance organic transistor memory elements with steep flanks of hysteresis. Adv Funct Mater, 2008, 18: 2593–2601
19 Jeong JW, Shin G, Park SI, *et al.* Soft materials in neuroengineering for hard problems in neuroscience. Neuron, 2015, 86: 175–186
20 Sekitani T, Someya T. Human-friendly organic integrated circuits. Mater Today, 2011, 14: 398–407
21 Bauer S, Bauer-gogonea S, Graz I, *et al.* 25th anniversary article: a soft future: from robots and sensor skin to energy harvesters. Adv Mater, 2014, 26: 149–162
22 Kim DH, Ahn JH, Choi WM, *et al.* Stretchable and foldable silicon integrated circuits. Science, 2008, 320: 507–511
23 Pan S, Lin H, Deng J, *et al.* Novel wearable energy devices based on aligned carbon nanotube fiber textiles. Adv Energy Mater, 2015, 5: 1401438
24 Pan S, Yang Z, Chen P, *et al.* Wearable solar cells by stacking textile electrodes. Angew Chem Int Ed, 2014, 53: 6110–6114
25 Kim DH, Ghaffari R, Lu N, *et al.* Flexible and stretchable electronics for biointegrated devices. Annu Rev Biomed Eng, 2012, 14: 113–128
26 Someya T, Kaltenbrunner M, Yokota T. Ultraflexible organic electronics. MRS Bull, 2015, 40: 1130–1137
27 Qian Y, Zhang X, Xie L, *et al.* Stretchable organic semiconductor devices. Adv Mater, 2016, doi: 10.1002/adma.201601278
28 Mannoor MS, Tao H, Clayton JD, *et al.* Graphene-based wireless bacteria detection on tooth enamel. Nat Commun, 2012, 3: 763
29 Drack M, Graz I, Sekitani T, *et al.* An imperceptible plastic electronic wrap. Adv Mater, 2015, 27: 34–40
30 Khodagholy D, Rivnay J, Sessolo M, *et al.* High transconductance organic electrochemical transistors. Nat Commun, 2013, 4: 2133
31 Gustafsson G, Cao Y, Treacy GM, *et al.* Flexible light-emitting diodes made from soluble conducting polymers. Nature, 1992, 357: 477–479
32 Garnier F, Hajlaoui R, Yassar A, *et al.* All-polymer field-effect transistor realized by printing techniques. Science, 1994, 265: 1684–1686
33 Gu G, Shen Z, Burrows PE, *et al.* Transparent flexible organic light-emitting devices. Adv Mater, 1997, 9: 725–728
34 Drury CJ, Mutsaers CMJ, Hart CM, *et al.* Low-cost all-polymer integrated circuits. Appl Phys Lett, 1998, 73: 108
35 Möller S, Perlov C, Jackson W, *et al.* A polymer/semiconductor write-once read-many-times memory. Nature, 2003, 426: 166–169
36 Aernouts T, Vanlaeke P, Geens W, *et al.* Printable anodes for flexible organic solar cell modules. Thin Solid Films, 2004, 451-452: 22–25
37 Kuribara K, Wang H, Uchiyama N, *et al.* Organic transistors with high thermal stability for medical applications. Nat Commun, 2012, 3: 723
38 Peng B, Ren X, Wang Z, *et al.* High performance organic transistor active-matrix driver developed on paper substrate. Sci Rep, 2014, 4: 6430
39 Fukuda K, Sekitani T, Zschieschang U, *et al.* A 4 V operation, flexible braille display using organic transistors, carbon nanotube actuators, and organic static random-access memory. Adv Funct Mater, 2011, 21: 4019–4027
40 Zschieschang U, Kang MJ, Takimiya K, *et al.* Flexible low-voltage organic thin-film transistors and circuits based on C_{10} -DNTT. J Mater Chem, 2012, 22: 4273–4277
41 Zhao B, He Z, Cheng X, *et al.* Flexible polymer solar cells with power conversion efficiency of 8.7%. J Mater Chem C, 2014, 2:

5077
42 Xiao B, Wu H, Cao Y. Solution-processed cathode interfacial layer materials for high-efficiency polymer solar cells. Mater Today, 2015, 18: 385–394
43 Jagadamma LK, Al-senani M, El-labban A, *et al.* Polymer solar cells with efficiency >10% enabled via a facile solution-processed Al-doped ZnO electron transporting layer. Adv Energy Mater, 2015, 5: 1500204
44 Xu J, Smith GM, Dun C, *et al.* Layered, nanonetwork composite cathodes for flexible, high-efficiency, organic light emitting devices. Adv Funct Mater, 2015, 25: 4397–4404
45 Han TH, Lee Y, Choi MR, *et al.* Extremely efficient flexible organic light-emitting diodes with modified graphene anode. Nat Photon, 2012, 6: 105–110
46 Zhou L, Xiang HY, Shen S, *et al.* High-performance flexible organic light-emitting diodes using embedded silver network transparent electrodes. ACS Nano, 2014, 8: 12796–12805
47 Xiang HY, Li YQ, Zhou L, *et al.* Outcoupling-enhanced flexible organic light-emitting diodes on ameliorated plastic substrate with built-in indium–tin-oxide-free transparent electrode. ACS Nano, 2015, 9: 7553–7562
48 Khan MA, Bhansali US, Alshareef HN. High-performance nonvolatile organic ferroelectric memory on banknotes. Adv Mater, 2012, 24: 2165–2170
49 Wang ZB, Helander MG, Hudson ZM, *et al.* Pt(II) complex based phosphorescent organic light emitting diodes with external quantum efficiencies above 20%. Appl Phys Lett, 2011, 98: 213301
50 Forrest SR. The path to ubiquitous and low-cost organic electronic appliances on plastic. Nature, 2004, 428: 911–918
51 Kim W, Kwon S, Lee SM, *et al.* Soft fabric-based flexible organic light-emitting diodes. Org Electron, 2013, 14: 3007–3013
52 Matsuhisa N, Kaltenbrunner M, Yokota T, *et al.* Printable elastic conductors with a high conductivity for electronic textile applications. Nat Commun, 2015, 6: 7461
53 Liu Y, Qi N, Song T, *et al.* Highly flexible and lightweight organic solar cells on biocompatible silk fibroin. ACS Appl Mater Interfaces, 2014, 6: 20670–20675
54 Zhu B, Wang H, Leow WR, *et al.* Silk fibroin for flexible electronic devices. Adv Mater, 2016, 28: 4250–4265
55 Tobjörk D, Österbacka R. Paper electronics. Adv Mater, 2011, 23: 1935–1961
56 Asadpoordarvish A, Sandström A, Larsen C, *et al.* Light-emitting paper. Adv Funct Mater, 2015, 25: 3238–3245
57 Fujisaki Y, Koga H, Nakajima Y, *et al.* Transparent nanopaper-based flexible organic thin-film transistor array. Adv Funct Mater, 2014, 24: 1657–1663
58 Zhang YZ, Wang Y, Cheng T, *et al.* Flexible supercapacitors based on paper substrates: a new paradigm for low-cost energy storage. Chem Soc Rev, 2015, 44: 5181–5199
59 Xie Z, Hung LS, Zhu F. A flexible top-emitting organic light-emitting diode on steel foil. Chem Phys Lett, 2003, 381: 691–696
60 Nagashima K, Koga H, Celano U, *et al.* Cellulose nanofiber paper as an ultra flexible nonvolatile memory. Sci Rep, 2014, 4:
61 Schauer S, Liu X, Worgull M, *et al.* Shape-memory polymers as flexible resonator substrates for continuously tunable organic DFB lasers. Opt Mater Express, 2015, 5: 576
62 Reeder J, Kaltenbrunner M, Ware T, *et al.* Mechanically adaptive organic transistors for implantable electronics. Adv Mater, 2014, 26: 4967–4973
63 Avendano-bolivar A, Ware T, Arreaga-salas D, *et al.* Mechanical cycling stability of organic thin film transistors on shape memory polymers. Adv Mater, 2013, 25: 3095–3099
64 Liu D, Zhao M, Li Y, *et al.* Solid-state, polymer-based fiber solar cells with carbon nanotube electrodes. ACS Nano, 2012, 6: 11027–11034
65 Wang X, Jiang K, Shen G. Flexible fiber energy storage and integrated devices: recent progress and perspectives. Mater Today, 2015, 18: 265–272
66 Zeng W, Shu L, Li Q, *et al.* Fiber-based wearable electronics: a review of materials, fabrication, devices, and applications. Adv Mater, 2014, 26: 5310–5336
67 Lee MR, Eckert RD, Forberich K, *et al.* Solar power wires based on organic photovoltaic materials. Science, 2009, 324: 232–235
68 Zhang Z, Yang Z, Deng J, *et al.* Stretchable polymer solar cell fibers. Small, 2015, 11: 675–680
69 Kwon S, Kim W, Kim H, *et al.* High luminance fiber-based polymer light-emitting devices by a dip-coating method. Adv Electron Mater, 2015, 1: 1500103
70 Park J, Kim J, Lee S, *et al.* Free-standing film electronics using photo-crosslinking layer-by-layer assembly. J Mater Chem, 2009, 19: 4488
71 Liang J, Li L, Tong K, *et al.* Silver nanowire percolation network soldered with graphene oxide at room temperature and its application for fully stretchable polymer light-emitting diodes. ACS Nano, 2014, 8: 1590–1600
72 Song M, Park JH, Kim CS, *et al.* Highly flexible and transparent conducting silver nanowire/ZnO composite film for organic solar cells. Nano Res, 2014, 7: 1370–1379
73 Bae S, Kim H, Lee Y, *et al.* Roll-to-roll production of 30-inch graphene films for transparent electrodes. Nat Nanotech, 2010, 5: 574–578
74 Na SI, Kim SS, Jo J, *et al.* Efficient and flexible ITO-free organic solar cells using highly conductive polymer anodes. Adv Mater, 2008, 20: 4061–4067
75 Gomez de arco L, Zhang Y, Schlenker CW, *et al.* Continuous, highly flexible, and transparent graphene films by chemical vapor deposition for organic photovoltaics. ACS Nano, 2010, 4: 2865–2873
76 Kim H, Horwitz JS, Kushto GP, *et al.* Indium tin oxide thin films grown on flexible plastic substrates by pulsed-laser deposition for organic light-emitting diodes. Appl Phys Lett, 2001, 79: 284
77 Zhu F, Zhang K, Guenther E, *et al.* Optimized indium tin oxide contact for organic light emitting diode applications. Thin Solid Films, 2000, 363: 314–317
78 Fang J, Matyba P, Edman L. The design and realization of flexible, long-lived light-emitting electrochemical cells. Adv Funct Mater, 2009, 19: 2671–2676
79 Hernandez-sosa G, Tekoglu S, Stolz S, *et al.* The compromises of printing organic electronics: a case study of gravure-printed light-emitting electrochemical cells. Adv Mater, 2014, 26: 3235–3240
80 Hu L, Hecht DS, Grüner G. Percolation in transparent and conducting carbon nanotube networks. Nano Lett, 2004, 4: 2513–2517
81 Dressel M, Gruner G. Electrodynamics of Solids: Optical Properties of Electrons in Matter. Cambridge: Cambridge University Press, 2002
82 De S, Lyons PE, Sorel S, *et al.* Transparent, flexible, and highly conductive thin films based on polymer–nanotube composites. ACS Nano, 2009, 3: 714–720
83 Vosgueritchian M, Lipomi DJ, Bao Z. Highly conductive and transparent PEDOT:PSS films with a fluorosurfactant for stretchable and flexible transparent electrodes. Adv Funct Mater, 2012, 22: 421–428
84 Do H, Reinhard M, Vogeler H, *et al.* Polymeric anodes from poly(3,4-ethylenedioxythiophene):poly(styrenesulfonate) for

3.5% efficient organic solar cells. Thin Solid Films, 2009, 517: 5900–5902
85 Levermore PA, Chen L, Wang X, *et al.* Fabrication of highly conductive poly(3,4-ethylenedioxythiophene) films by vapor phase polymerization and their application in efficient organic light-emitting diodes. Adv Mater, 2007, 19: 2379–2385
86 Lipomi DJ, Tee BCK, Vosgueritchian M, *et al.* Stretchable organic solar cells. Adv Mater, 2011, 23: 1771–1775
87 Tait JG, Worfolk BJ, Maloney SA, *et al.* Spray coated high-conductivity PEDOT:PSS transparent electrodes for stretchable and mechanically-robust organic solar cells. Solar Energy Mater Solar Cells, 2013, 110: 98–106
88 Nagata R, Yanagi Y, Fujii S, *et al.* Highly conductive DMSO-treated PEDOT:PSS electrodes applied to flexible organic solar cells. IEICE Trans Electron, 2015, E98.C: 411–421
89 Seo KW, Lee JH, Kim HJ, *et al.* Highly transparent and flexible InTiO/Ag nanowire/InTiO films for flexible organic solar cells. Appl Phys Lett, 2014, 105: 031911
90 http://clevios.com/en/applications/highlyconductiveclevios/highly-conductive-clevios.aspx PbCPm, Haraeus
91 Lipomi DJ, Lee JA, Vosgueritchian M, *et al.* Electronic properties of transparent conductive films of PEDOT:PSS on stretchable substrates. Chem Mater, 2012, 24: 373–382
92 Kim YH, Sachse C, Machala ML, *et al.* Highly conductive PEDOT:PSS electrode with optimized solvent and thermal post-treatment for ITO-free organic solar cells. Adv Funct Mater, 2011, 21: 1076–1081
93 Saghaei J, Fallahzadeh A, Saghaei T. ITO-free organic solar cells using highly conductive phenol-treated PEDOT:PSS anodes. Org Electron, 2015, 24: 188–194
94 Xia Y, Sun K, Ouyang J. Solution-processed metallic conducting polymer films as transparent electrode of optoelectronic devices. Adv Mater, 2012, 24: 2436–2440
95 Fan X, Wang J, Wang H, *et al.* Bendable ITO-free organic solar cells with highly conductive and flexible PEDOT:PSS electrodes on plastic substrates. ACS Appl Mater Interfaces, 2015, 7: 16287–16295
96 Kaltenbrunner M, White MS, Głowacki ED, *et al.* Ultrathin and lightweight organic solar cells with high flexibility. Nat Commun, 2012, 3: 770
97 Kaltenbrunner M, Adam G, Głowacki ED, *et al.* Flexible high power-per-weight perovskite solar cells with chromium oxide–metal contacts for improved stability in air. Nat Mater, 2015, 14: 1032–1039
98 Zhou Y, Fuentes-hernandez C, Shim J, *et al.* A universal method to produce low-work function electrodes for organic electronics. Science, 2012, 336: 327–332
99 Liu J, Xie L, Huang W. Transparent, conductive, and flexible graphene films from large-size graphene oxide. Integrated Ferroelectrics, 2011, 128: 105–109
100 Fan TJ, Yuan CQ, Tang W, *et al.* A novel method of fabricating flexible transparent conductive large area graphene film. Chin Phys Lett, 2015, 32: 076802
101 Rowell MW, Topinka MA, Mcgehee MD, *et al.* Organic solar cells with carbon nanotube network electrodes. Appl Phys Lett, 2006, 88: 233506
102 Son SY, Yun JM, Noh YJ, *et al.* Highly flexible and bendable carbon nanosheets as transparent conducting electrodes for organic solar cells. Carbon, 2015, 81: 546–551
103 Lee S, Yeo JS, Ji Y, *et al.* Flexible organic solar cells composed of P3HT:PCBM using chemically doped graphene electrodes. Nanotechnology, 2012, 23: 344013
104 Yin Z, Sun S, Salim T, *et al.* Organic photovoltaic devices using highly flexible reduced graphene oxide films as transparent electrodes. ACS Nano, 2010, 4: 5263–5268
105 Kymakis E, Savva K, Stylianakis MM, *et al.* Flexible organic photovoltaic cells with *in situ* nonthermal photoreduction of spin-coated graphene oxide electrodes. Adv Funct Mater, 2013, 23: 2742–2749
106 Hu L, Gruner G, Gong J, *et al.* Electrowetting devices with transparent single-walled carbon nanotube electrodes. Appl Phys Lett, 2007, 90: 093124
107 Li J, Hu L, Wang L, *et al.* Organic light-emitting diodes having carbon nanotube anodes. Nano Lett, 2006, 6: 2472–2477
108 Cho DY, Eun K, Choa SH, *et al.* Highly flexible and stretchable carbon nanotube network electrodes prepared by simple brush painting for cost-effective flexible organic solar cells. Carbon, 2014, 66: 530–538
109 Jeon I, Cui K, Chiba T, *et al.* Direct and dry deposited single-walled carbon nanotube films doped with MoO_x as electron-blocking transparent electrodes for flexible organic solar cells. J Am Chem Soc, 2015, 137: 7982–7985
110 Yang Z, Deng J, Sun H, *et al.* Self-powered energy fiber: energy conversion in the sheath and storage in the core. Adv Mater, 2014, 26: 7038–7042
111 Liu ZD, Yin ZY, Du ZH, *et al.* Low temperature growth of graphene on Cu–Ni alloy nanofibers for stable, flexible electrodes. Nanoscale, 2014, 6: 5110
112 Kim KS, Zhao Y, Jang H, *et al.* Large-scale pattern growth of graphene films for stretchable transparent electrodes. Nature, 2009, 457: 706–710
113 Lipomi DJ, Vosgueritchian M, Tee BCK, *et al.* Skin-like pressure and strain sensors based on transparent elastic films of carbon nanotubes. Nat Nanotech, 2011, 6: 788–792
114 Nam S, Song M, Kim DH, *et al.* Ultrasmooth, extremely deformable and shape recoverable Ag nanowire embedded transparent electrode. Sci Rep, 2014, 4:
115 Hu L, Kim HS, Lee JY, *et al.* Scalable coating and properties of transparent, flexible, silver nanowire electrodes. ACS Nano, 2010, 4: 2955–2963
116 Jin H, Tao C, Velusamy M, *et al.* Efficient, large area ITO-and-PEDOT-free organic solar cell sub-modules. Adv Mater, 2012, 24: 2572–2577
117 Yun J, Wang W, Bae TS, *et al.* Preparation of flexible organic solar cells with highly conductive and transparent metal-oxide multilayer electrodes based on silver oxide. ACS Appl Mater Interfaces, 2013, 5: 9933–9941
118 Lee JY, Connor ST, Cui Y, *et al.* Solution-processed metal nanowire mesh transparent electrodes. Nano Lett, 2008, 8: 689–692
119 Kang SB, Noh YJ, Na SI, *et al.* Brush-painted flexible organic solar cells using highly transparent and flexible Ag nanowire network electrodes. Solar Energy Mater Solar Cells, 2014, 122: 152–157
120 Yu Z, Zhang Q, Li L, *et al.* Highly flexible silver nanowire electrodes for shape-memory polymer light-emitting diodes. Adv Mater, 2011, 23: 664–668
121 De S, Higgins TM, Lyons PE, *et al.* Silver nanowire networks as flexible, transparent, conducting films: extremely high DC to optical conductivity ratios. ACS Nano, 2009, 3: 1767–1774
122 Triambulo RE, Cheong HG, Park JW. All-solution-processed foldable transparent electrodes of Ag nanowire mesh and metal matrix films for flexible electronics. Org Electron, 2014, 15: 2685–2695
123 Kim Y, Ryu TI, Ok KH, *et al.* Inverted layer-by-layer fabrication of an ultraflexible and transparent Ag nanowire/conductive polymer composite electrode for use in high-performance organic solar cells. Adv Funct Mater, 2015, 25: 4580–4589
124 Jung S, Lee S, Song M, *et al.* Extremely flexible transparent con-

ducting electrodes for organic devices. Adv Energy Mater, 2014, 4: 1300474
125 Cheng T, Zhang YZ, Lai WY, *et al.* High-performance stretchable transparent electrodes based on silver nanowires synthesized via an eco-friendly halogen-free method. J Mater Chem C, 2014, 2: 10369–10376
126 Chen J, Zhou W, Chen J, *et al.* Solution-processed copper nanowire flexible transparent electrodes with PEDOT:PSS as binder, protector and oxide-layer scavenger for polymer solar cells. Nano Res, 2015, 8: 1017–1025
127 Keplinger C, Sun JY, Foo CC, *et al.* Stretchable, transparent, ionic conductors. Science, 2013, 341: 984–987
128 Cheong HG, Triambulo RE, Lee GH, *et al.* Silver nanowire network transparent electrodes with highly enhanced flexibility by welding for application in flexible organic light-emitting diodes. ACS Appl Mater Interfaces, 2014, 6: 7846–7855
129 Tekoglu S, Hernandez-sosa G, Kluge E, *et al.* Gravure printed flexible small-molecule organic light emitting diodes. Org Electron, 2013, 14: 3493–3499
130 Melpignano P, Biondo V, Sinesi S, *et al.* Efficient light extraction and beam shaping from flexible, optically integrated organic light-emitting diodes. Appl Phys Lett, 2006, 88: 153514
131 Luo Y, Wang C, Wang L, *et al.* Flexible organic light-emitting diodes with enhanced light out-coupling efficiency fabricated on a double-sided nanotextured substrate. ACS Appl Mater Interfaces, 2014, 6: 10213–10219
132 Wang R, Xu LH, Li YQ, *et al.* Broadband light out-coupling enhancement of flexible organic light-emitting diodes using biomimetic quasirandom nanostructures. Advanced Optical Mater, 2015, 3: 203–210
133 Lee SM, Cho Y, Kim DY, *et al.* Enhanced light extraction from mechanically flexible, nanostructured organic light-emitting diodes with plasmonic nanomesh electrodes. Advanced Optical Mater, 2015, 3: 1240–1247
134 Kim E, Cho H, Kim K, *et al.* A facile route to efficient, low-cost flexible organic light-emitting diodes: utilizing the high refractive index and built-in scattering properties of industrial-grade PEN substrates. Adv Mater, 2015, 27: 1624–1631
135 Liu B, Wang L, Xu M, *et al.* Extremely stable-color flexible white organic light-emitting diodes with efficiency exceeding 100 lm W^{-1}. J Mater Chem C, 2014, 2: 9836–9841
136 Salinas JF, Yip HL, Chueh CC, *et al.* Optical design of transparent thin metal electrodes to enhance in-coupling and trapping of light in flexible polymer solar cells. Adv Mater, 2012, 24: 6362–6367
137 Chang HW, Lee J, Hofmann S, *et al.* Nano-particle based scattering layers for optical efficiency enhancement of organic light-emitting diodes and organic solar cells. J Appl Phys, 2013, 113: 204502
138 Sergeant NP, Niesen B, Liu AS, *et al.* Resonant cavity enhanced light harvesting in flexible thin-film organic solar cells. Opt Lett, 2013, 38: 1431
139 Wang BY, Yoo TH, Lim JW, *et al.* Enhanced light scattering and trapping effect of ag nanowire mesh electrode for high efficient flexible organic solar cell. Small, 2015, 11: 1905–1911
140 Yun J, Wang W, Kim SM, *et al.* Light trapping in bendable organic solar cells using silica nanoparticle arrays. Energy Environ Sci, 2015, 8: 932–940
141 Park SI, Ahn JH, Feng X, *et al.* Theoretical and experimental studies of bending of inorganic electronic materials on plastic substrates. Adv Funct Mater, 2008, 18: 2673–2684
142 Sekitani T, Iba S, Kato Y, *et al.* Ultraflexible organic field-effect transistors embedded at a neutral strain position. Appl Phys Lett, 2005, 87: 173502
143 Sekitani T, Zschieschang U, Klauk H, *et al.* Flexible organic transistors and circuits with extreme bending stability. Nat Mater, 2010, 9: 1015–1022
144 Reuveny A, Yokota T, Sekitani T, *et al.* Ultra-flexible short-channel organic field-effect transistors. Appl Phys Express, 2015, 8: 091601
145 Fukuda K, Takeda Y, Yoshimura Y, *et al.* Fully-printed high-performance organic thin-film transistors and circuitry on one-micron-thick polymer films. Nat Commun, 2014, 5:
146 White MS, Kaltenbrunner M, Głowacki ED, *et al.* Ultrathin, highly flexible and stretchable PLEDs. Nat Photon, 2013, 7: 811–816
147 Liang J, Li L, Niu X, *et al.* Elastomeric polymer light-emitting devices and displays. Nat Photon, 2013, 7: 817–824
148 List kratochvil EJW, Cosseddu P, Casula G, *et al.* SPIE proceedings. 2015, 9569: 956906
149 Bonfiglio A, Mameli F, Sanna O. A completely flexible organic transistor obtained by a one-mask photolithographic process. Appl Phys Lett, 2003, 82: 3550
150 Yi HT, Payne MM, Anthony JE, *et al.* Ultra-flexible solution-processed organic field-effect transistors. Nat Commun, 2012, 3: 1259
151 Zhang L, Wang H, Zhao Y, *et al.* Substrate-free ultra-flexible organic field-effect transistors and five-stage ring oscillators. Adv Mater, 2013, 25: 5455–5460
152 Sekitani T, Iba S, Kato Y, *et al.* Submillimeter radius bendable organic field-effect transistors. J Non-Crystalline Solids, 2006, 352: 1769–1773
153 Crone B, Dodabalapur A, Lin YY, *et al.* Large-scale complementary integrated circuits based on organic transistors. Nature, 2000, 403: 521–523
154 Dodabalapur A. Organic and polymer transistors for electronics. Mater Today, 2006, 9: 24–30
155 Uno M, Nakayama K, Soeda J, *et al.* High-speed flexible organic field-effect transistors with a 3D structure. Adv Mater, 2011, 23: 3047–3051
156 Zschieschang U, Yamamoto T, Takimiya K, *et al.* Organic electronics on banknotes. Adv Mater, 2011, 23: 654–658
157 Fukuda K, Takeda Y, Mizukami M, *et al.* Fully solution-processed flexible organic thin film transistor arrays with high mobility and exceptional uniformity. Sci Rep, 2014, 4:
158 Dong J, Chai YH, Zhao YZ, *et al.* The progress of flexible organic field-effect transistors. Acta Phys Sin, 2013, 62: 047301
159 Jedaa A, Halik M. Toward strain resistant flexible organic thin film transistors. Appl Phys Lett, 2009, 95: 103309
160 Kaltenbrunner M, Sekitani T, Reeder J, *et al.* An ultra-lightweight design for imperceptible plastic electronics. Nature, 2013, 499: 458–463
161 Lee S, Reuveny A, Reeder J, *et al.* A transparent bending-insensitive pressure sensor. Nat Nanotech, 2016, 11: 472–478
162 Reuveny A, Lee S, Yokota T, *et al.* High-frequency, conformable organic amplifiers. Adv Mater, 2016, 28: 3298–3304
163 Yi M, Guo Y, Guo J, *et al.* The mechanical bending effect and mechanism of high performance and low-voltage flexible organic thin-film transistors with a cross-linked PVP dielectric layer. J Mater Chem C, 2014, 2: 2998
164 Zang Y, Zhang F, Huang D, *et al.* Flexible suspended gate organic thin-film transistors for ultra-sensitive pressure detection. Nat Commun, 2015, 6: 6269
165 Zhang L, Di C, Zhao Y, *et al.* Top-gate organic thin-film transistors constructed by a general lamination approach. Adv Mater, 2010, 22: 3537–3541
166 Nawrocki RA, Matsuhisa N, Yokota T, *et al.* 300-nm imperceptible, ultraflexible, and biocompatible e-skin fit with tactile sensors and organic transistors. Adv Electron Mater, 2016, 2: 1500452

167 Someya T, Sekitani T, Iba S, *et al.* A large-area, flexible pressure sensor matrix with organic field-effect transistors for artificial skin applications. Proc Natl Acad Sci USA, 2004, 101: 9966–9970
168 Liu Z, Qi D, Guo P, *et al.* Thickness-gradient films for high gauge factor stretchable strain sensors. Adv Mater, 2015, 27: 6230–6237
169 Kim T, Kim JH, Kang TE, *et al.* Flexible, highly efficient all-polymer solar cells. Nat Commun, 2015, 6: 8547
170 Gu G, Burrows PE, Venkatesh S, *et al.* Vacuum-deposited, non-polymeric flexible organic light-emitting devices. Opt Lett, 1997, 22: 172
171 Wang ZB, Helander MG, Qiu J, *et al.* Unlocking the full potential of organic light-emitting diodes on flexible plastic. Nat Photon, 2011, 5: 753–757
172 Park JS, Kim TW, Stryakhilev D, *et al.* Flexible full color organic light-emitting diode display on polyimide plastic substrate driven by amorphous indium gallium zinc oxide thin-film transistors. Appl Phys Lett, 2009, 95: 013503
173 Wang Y, Liu S, Dang F, *et al.* An efficient flexible white organic light-emitting device with a screen-printed conducting polymer anode. J Phys D-Appl Phys, 2012, 45: 402002
174 Zhang D, Ryu K, Liu X, *et al.* Transparent, conductive, and flexible carbon nanotube films and their application in organic light-emitting diodes. Nano Lett, 2006, 6: 1880–1886
175 Liu YF, Feng J, Cui HF, *et al.* Fabrication and characterization of Ag film with sub-nanometer surface roughness as a flexible cathode for inverted top-emitting organic light-emitting devices. Nanoscale, 2013, 5: 10811
176 Liu S, Liu W, Yu J, *et al.* Silver/germanium/silver: an effective transparent electrode for flexible organic light-emitting devices. J Mater Chem C, 2014, 2: 835–840
177 Duan YH, Duan Y, Wang X, *et al.* Highly flexible peeled-off silver nanowire transparent anode using in organic light-emitting devices. Appl Surface Sci, 2015, 351: 445–450
178 Cho H, Yun C, Park JW, *et al.* Highly flexible organic light-emitting diodes based on ZnS/Ag/WO3 multilayer transparent electrodes. Org Electron, 2009, 10: 1163–1169
179 Lewis J, Grego S, Chalamala B, *et al.* Highly flexible transparent electrodes for organic light-emitting diode-based displays. Appl Phys Lett, 2004, 85: 3450
180 Wu C, Li F, Wu W, *et al.* Liquid-phase exfoliation of chemical vapor deposition-grown single layer graphene and its application in solution-processed transparent electrodes for flexible organic light-emitting devices. Appl Phys Lett, 2014, 105: 243509
181 Wang L, Swensen JS, Polikarpov E, *et al.* Highly efficient blue organic light-emitting devices with indium-free transparent anode on flexible substrates. Org Electron, 2010, 11: 1555–1560
182 Chen S, Zhao X, Wu Q, *et al.* Efficient, color-stable flexible white top-emitting organic light-emitting diodes. Org Electron, 2013, 14: 3037–3045
183 Chen SF, Guo X, Wu Q, *et al.* Flexible white top-emitting organic light-emitting diode with a MoO_x roughness improvement layer. Chin Phys B, 2013, 22: 128506
184 Shi H, Deng L, Chen S, *et al.* High performance flexible top-emitting warm-white organic light-emitting devices and chromaticity shift mechanism. AIP Adv, 2014, 4: 047110
185 Shi H, Deng L, Chen S, *et al.* Flexible top-emitting warm-white organic light-emitting diodes with highly luminous performances and extremely stable chromaticity. Org Electron, 2014, 15: 1465–1475
186 Zhu H, Xiao Z, Liu D, *et al.* Biodegradable transparent substrates for flexible organic-light-emitting diodes. Energy Environ Sci, 2013, 6: 2105
187 Li L, Yu Z, Hu W, *et al.* Efficient flexible phosphorescent polymer light-emitting diodes based on silver nanowire-polymer composite electrode. Adv Mater, 2011, 23: 5563–5567
188 Yokota T, Zalar P, Kaltenbrunner M, *et al.* Ultraflexible organic photonic skin. Sci Adv, 2016, 2: e1501856–e1501856
189 Kim S, Kwon HJ, Lee S, *et al.* Low-power flexible organic light-emitting diode display device. Adv Mater, 2011, 23: 3511–3516
190 Yun SO, Hwang Y, Park J, *et al.* Sticker-type Alq_3 -based OLEDs based on printable ultrathin substrates in periodically anchored and suspended configurations. Adv Mater, 2013, 25: 5626–5631
191 Kwon HJ, Shim HS, Kim S, *et al.* Mechanically and optically reliable folding structure with a hyperelastic material for seamless foldable displays. Appl Phys Lett, 2011, 98: 151904
192 Kim S, Choi W, Rim W, *et al.* A highly sensitive capacitive touch sensor integrated on a thin-film-encapsulated active-matrix OLED for ultrathin displays. IEEE Trans Electron Devices, 2011, 58: 3609–3615
193 Wang C, Hwang D, Yu Z, *et al.* User-interactive electronic skin for instantaneous pressure visualization. Nat Mater, 2013, 12: 899–904
194 Bauer S. Flexible electronics: sophisticated skin. Nat Mater, 2013, 12: 871–872
195 Lin WP, Liu SJ, Gong T, *et al.* Polymer-based resistive memory materials and devices. Adv Mater, 2014, 26: 570–606
196 Islam SM, Banerji P, Banerjee S. Electrical bistability, negative differential resistance and carrier transport in flexible organic memory device based on polymer bilayer structure. Org Electron, 2014, 15: 144–149
197 Raeis hosseini N, Lee JS. Resistive switching memory based on bioinspired natural solid polymer electrolytes. ACS Nano, 2015, 9: 419–426
198 Lai YC, Wang YX, Huang YC, *et al.* Rewritable, moldable, and flexible sticker-type organic memory on arbitrary substrates. Adv Funct Mater, 2014, 24: 1430–1438
199 Liu J, Zeng Z, Cao X, *et al.* Preparation of MoS_2 -polyvinylpyrrolidone nanocomposites for flexible nonvolatile rewritable memory devices with reduced graphene oxide electrodes. Small, 2012, 8: 3517–3522
200 Ji Y, Cho B, Song S, *et al.* Stable switching characteristics of organic nonvolatile memory on a bent flexible substrate. Adv Mater, 2010, 22: 3071–3075
201 Jung SW, Choi JS, Koo JB, *et al.* Flexible nonvolatile organic ferroelectric memory transistors fabricated on polydimethylsiloxane elastomer. Org Electron, 2015, 16: 46–53
202 Kaltenbrunner M, Stadler P, Schwödiauer R, *et al.* Anodized aluminum oxide thin films for room-temperature-processed, flexible, low-voltage organic non-volatile memory elements with excellent charge retention. Adv Mater, 2011, 23: 4892–4896
203 Kim SJ, Lee JS. Flexible organic transistor memory devices. Nano Lett, 2010, 10: 2884–2890
204 Zhang L, Wu T, Guo Y, *et al.* Large-area, flexible imaging arrays constructed by light-charge organic memories. Sci Rep, 2013, 3:
205 Kim SJ, Song JM, Lee JS. Transparent organic thin-film transistors and nonvolatile memory devices fabricated on flexible plastic substrates. J Mater Chem, 2011, 21: 14516
206 Hwang SK, Park TJ, Kim KL, *et al.* Organic one-transistor-type nonvolatile memory gated with thin ionic liquid-polymer film for low voltage operation. ACS Appl Mater Interfaces, 2014, 6: 20179–20187
207 Kang M, Khim D, Park WT, *et al.* Synergistic high charge-storage capacity for multi-level flexible organic flash memory. Sci Rep, 2015, 5: 12299
208 Chai YH, Guo YX, Bian W, *et al.* Progress of flexible organic non-

volatile memory field-effect transistors. Acta Phys Sin, 2014, 63: 27302
209 Jeong JW, Yeo WH, Akhtar A, *et al.* Materials and optimized designs for human-machine interfaces via epidermal electronics. Adv Mater, 2013, 25: 6839–6846
210 Jung SW, Na BS, Park CW, *et al.* Low-voltage-operated organic one-time programmable memory using printed organic thin-film transistors and antifuse capacitors. J Nanosci Nanotechnol, 2014, 14: 8167–8170
211 Han ST, Zhou Y, Roy VAL. Towards the development of flexible non-volatile memories. Adv Mater, 2013, 25: 5425–5449
212 Sekitani T, Yokota T, Zschieschang U, *et al.* Organic nonvolatile memory transistors for flexible sensor arrays. Science, 2009, 326: 1516–1519
213 Nau S, Wolf C, Sax S, *et al.* Organic non-volatile resistive photoswitches for flexible image detector arrays. Adv Mater, 2015, 27: 1048–1052
214 Zhu B, Wang H, Liu Y, *et al.* Skin-inspired haptic memory arrays with an electrically reconfigurable architecture. Adv Mater, 2016, 28: 1559–1566
215 Huang R, Cai Y, Liu Y, *et al.* Resistive switching in organic memory devices for flexible applications. 2014 IEEE ISCAS, 2014, 838–841
216 Lee MJ, Park Y, Suh DS, *et al.* Two series oxide resistors applicable to high speed and high density nonvolatile memory. Adv Mater, 2007, 19: 3919–3923
217 Hong AJ, Song EB, Yu HS, *et al.* Graphene flash memory. ACS Nano, 2011, 5: 7812–7817
218 Kim RH, Kim HJ, Bae I, *et al.* Non-volatile organic memory with sub-millimeter bending radius. Nat Commun, 2014, 5: 3583
219 Cosseddu P, Lai S, Casula G, *et al.* High performance, foldable, organic memories based on ultra-low voltage, thin film transistors. Org Electron, 2014, 15: 3595–3600
220 Song S, Jang J, Ji Y, *et al.* Twistable nonvolatile organic resistive memory devices. Org Electron, 2013, 14: 2087–2092
221 http://www.prnewswire.com/news-releases/royole-develops-worlds-thinnest-001-mm-full-color-amoled-flexible-display-300010265.html

Acknowledgments This work was suppoted by the National Basic Research Program (2014CB648300), the National High Technology Research and Development Program of China (2011AA050526), the National Natural Science Foundation of China (21373114 and 21573111), a project funded by the Priority Academic Program Development of Jiangsu Higher Education Institutions (YX03001), Jiangsu National Synergetic Innovation Center for Advanced Materials (SICAM), Synergetic Innovation Center for Organic Electronics and Information Displays, the Natural Science Foundation of Jiangsu Province (BM2012010 and BE2011191), Excellent science and technology innovation team of Jiangsu Higher Education Institutions (2013), Qing Lan Project and NUPT 1311 project for their financial support. X Chen thanks the financial support from Singapore Ministry of Education Tier-2 (ARC26/15) and NTU-A*STAR Silicon Technologies Centre of Excellence (11235100003).

Author contributions Chen X and Huang W provided the overall concept and revised manuscript. Qian Y drafted the manuscript. Zhang X, Qi D, Xie L and Chandran BK participated in writing and critically revising the manuscript.

Conflict of interest The authors declare that they have no conflict of interest.

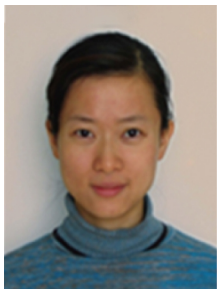

Yan Qian is an Associate Professor at Nanjing University of Posts & Telecommunications. She received her BSc degree in chemistry from Anhui University (China) in 2002 and PhD degree in chemistry from the Institute of Chemistry, Chinese Academy of Sciences in 2007. Since then, she has been worked at the Institute of Advanced Materials, Nanjing University of Posts & Telecommunications. Her research interests include design of organic opto/electronic functional materials and investigation of their structure-property relationship, especially organic photophysics.

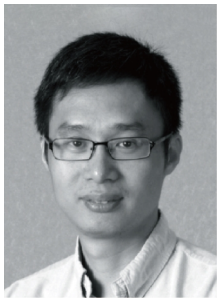

Xiaodong Chen is an Associate Professor at Nanyang Technological University, Singapore. He received his BSc degree in chemistry from Fuzhou University (China) in 1999, MSc degree in physical chemistry from the Chinese Academy of Sciences in 2002, and PhD degree in biochemistry from the University of Muenster (Germany) in 2006. After working as a postdoctoral fellow at the Northwestern University (USA), he started his independent research career as a Singapore National Research Foundation Fellow and Nanyang Assistant Professor at Nanyang Technological University in 2009. He was promoted to Associate Professor in September of 2013. His research interests include programmable materials for energy con-version, flexible/stretchable devices and integrated nano-bio interfaces.

Wei Huang received his PhD degree from Peking University in 1992. In 1993, he began his postdoctoral research at the National University of Singapore. In 2001, he was appointed as a chair professor of Fudan University, where he founded and chaired the Institute of Advanced Materials (IAM). In 2006, he was appointed vice president of Nanjing University of Posts and Telecommunications. Now, he is the president of Nanjing Tech University. He was elected as Academician of the Chinese Academy of Sciences in 2011. His research interests include organic/plastic materials and devices, nanomaterials, and nanotechnology.

超柔性薄膜有机半导体器件: 从柔性到超柔性

钱妍[1], 张新稳[1], 齐殿鹏[2], 解令海[1], Bevita K. Chandran[2], 陈晓东[2*], 黄维[1,3*]

摘要 柔性薄膜有机半导体器件由于其轻便、柔性、有机半导体的可重复制备及易于进行功能性调节、以及低成本、大面积溶液加工等特性而受到广泛关注. 其中, 弯曲半径不超过1 mm的超柔性电子对可折叠/便携设备、可穿戴设备、表皮及植入式电子设备、三维表面贴合型器件以及仿生学等领域的发展至关重要. 本综述首先简要介绍了从柔性到超柔性电子的发展史以及超柔性有机器件的设计. 接着, 聚焦于超柔性的有机场效应管、有机发光二极管、有机太阳能电池以及有机存储器等有机半导体功能器件领域的最新进展进行了总结评述.